Modelling and numerical methods in quantum kinetic theory

Weizhu Bao[1], Lorenzo Pareschi[2] and Peter A.Markowich[3]

[1] Department of Computational Science, National University of Singapore, Singapore 117543 bao@cz3.nus.edu.sg
[2] Department of Mathematics, University of Ferrara, Via Machiavelli 35, 4110 Ferrara Italy pareschi@dm.unife.it
[3] Institute of Mathematics, University of Vienna, Boltzmanngasse 9, 1090 Vienna, Austria Peter.Markowich@univie.ac.at

Summary. In this work we review some modelling and numerical aspects in quantum kinetic theory for a gas of interacting bosons and we will try to explain what makes Bose-Einstein condensation in a dilute gas mathematically interesting and numerically challenging. A particular care is devoted to the development of efficient numerical schemes for the quantum Boltzmann equation that preserve the main physical features of the continuous problem, namely conservation of mass and energy, the entropy inequality and generalized Bose-Einstein distributions as steady states. These properties are essential in order to develop numerical methods that are able to capture the challenging phenomenon of bosons condensation. We also show that the resulting schemes can be evaluated with the use of fast algorithms. In order to study the evolution of the condensate wave function the Gross-Pitaevskii equation is also presented together with some schemes for its efficient numerical solution.

1 Introduction

The quantum dynamics of many body systems is often modelled by a nonlinear Boltzmann equation which exhibits a particle-like collision behavior. The application of quantum assumptions to molecular encounters leads to some divergences from the classical kinetic theory[15] and despite their formal analogies the Boltzmann equation for classical and quantum kinetic theory present very different features.

The interest in the quantum framework of the Boltzmann equation has increased dramatically in the recent years. Although the quantum Boltzmann equation, or QBE, for a single specie of particles is valid for a gas of fermions as well as for a gas of bosons blow up of the solution in finite time may occur only in the latter case. As a consequence the QBE for a gas of bosons represents the most challenging case both mathematically and numerically. In particular this

equation has been successfully used for computing non-equilibrium situations where Bose-Einstein condensate occurs.

Bose-Einstein condensation, or BEC, has a long history dating from the early 1920s (see [11],[19],[20]). The notion of Bose statistics dates back to a 1924 paper in which Bose used a statistical argument to derive the black-body photon spectrum. Bose was unable to publish his work, so he sent it to Einstein who translated it into German and got it published. Einstein then extended the idea of Bose statistics to the case of noninteracting atoms. The result was Bose-Einstein statistics. Einstein noticed a peculiar feature of the distribution of the atoms over the quantized energy levels predicted by these statistics. At very low but finite temperature a large fraction of the atoms would go into the lowest energy quantum state. This phenomenon is now called Bose-Einstein condensation. The condition for BEC is that the phase space density must be greater than approximately unity, in natural units. Another way to express this is that the de Broglie wavelength of each atoms must be large enough to overlap with its neighbor.

Although it was a source of debate for decades, it is now recognized that the remarkable properties of superconductivity and superfluidity in both helium 3 and helium 4 are related to BEC. The appeal of superconductivity and of superfluidity, along with that of laser light, the third common system in which macroscopic quantum behavior is evident, provided the main motivation to the study of BEC in a gas. Experimentally this has been achieved thanks to strong advancements in trapping and cooling techniques for neutral atoms leading to the 2001 Nobel prize in physics by Cornell, Ketterle and Wiemann [16, 33].

A different description is provided by the time dependent Gross-Pitaevskii equation, or GPE, which can be viewed as an equation for the condensate wave function (order parameter for the Bose condensate)[28, 29]. This equation is a simplified description in that it includes no quantum fluctuations, or thermal or irreversible effects, but it may well be valid in the situation of a large number of condensate particles. Both of these equations contain essential aspects of the problem. However, in practice the process of creating a Bose-Einstein condensate in a trap by means of evaporative cooling starts in a regime covered by the QBE and finishes in a regime where the GPE is thought to be valid.

In the first part of this paper is to briefly recall the main properties of the QBE and to derive accurate numerical discretizations, which maintain the basic analytical and physical features of the continuous problem, namely, mass and energy conservation, entropy growth and equilibrium distributions. Although our treatment is valid for both fermions and bosons since we are interested in methods capable to describe the formation of condensate we will mainly concentrate on a gas of bosons. To this aim we consider the homogeneous Boltzmann equation for a quantum gas and derive first and second order accurate quadrature formulas for the collision operator in some relevant particular cases. These schemes due to their 'direct' derivation from the continuous operator possess all the desired physical properties at a discrete

level. In addition we show that with a suitable choice of the interacting kernel the computations can be performed with fast algorithms. Next we extend our method to the more general case of time dependent trap potentials [31].

For the sake of completeness we mention the recent works [14, 36, 41, 42, 43] in which fast methods for Boltzmann equations were derived using different techniques like multipole methods, multigrid methods and spectral methods. For a mathematical analysis of the quantum Boltzmann equation in the space homogeneous isotropic case we refer to [38, 39, 22, 23, 24]. We remark that already the issue of giving mathematical sense to the collision operator is highly nontrivial (particularly if positive measure solutions are allowed, as required by a careful analysis of the equilibrium states). Derivations of the QBE from the evolution of interacting quantum particles are found in [10, 21, 26]. Finally we mention here a recent paper by Buet and Cordier [13] where the asymptotic Kompaneets equation limit of the QBE has been studied numerically.

In the second part, in order to study the evolution of the condensate wave function, the Gross-Pitaevskii equation [30, 44] is also presented together with some schemes for its efficient numerical solution. Here we briefly review the time-splitting spectral method introduced in [5, 3, 2] and its main properties. A mathematical model for coupling QBE and GPE is also introduced [50].

The rest of the work is organized as follows. In the next Section we will introduce the QBE for bosons and its main physical properties. Next in Section 3 we discuss the details of our numerical schemes and some numerical examples are performed. The results confirm the capability of the methods to capture the concentration behavior of bosons. In Section 4 we extend the method to the case of time dependent trapping potentials. The GPE equation is then discussed in Section 5 together with its numerical solution. Finally in Section 6 some future directions of research and possible strategies for numerically coupling QBE and GPE are outlined.

2 The quantum Boltzmann equation

We consider a gas of interacting bosons, which are trapped by a confining potential $V = V(\mathbf{x})$ with $\min V(\mathbf{x}) = 0$. We denote the total energy of a boson with momentum $\mathbf{p} = (p_1, p_2, p_3)$ and position $\mathbf{x} = (x, y, z)$ (after an appropriate non-dimensionalization) by

$$\varepsilon(\mathbf{x}, \mathbf{p}) = \frac{|\mathbf{p}|^2}{2} + V(\mathbf{x}). \tag{1}$$

Let $F = F(\mathbf{x}, \mathbf{p}, t) \geq 0$ be the phase-space density of bosons.

2.1 The QBE in energy space

Assuming a boson distribution which only depends on the total energy ε we write

$$F(\mathbf{x},\mathbf{p},t) = f\left(\frac{|\mathbf{p}|^2}{2} + V(\mathbf{x}), t\right), \tag{2}$$

where $f = f(\varepsilon, t) \geq 0$ is the boson density in energy space.

Following [45, 46, 25, 26, 27] we write a Boltzmann-type equation (referred to as boson Boltzmann equation in the sequel) in energy space

$$\rho(\varepsilon)\frac{\partial f}{\partial t} = Q(f)(\varepsilon), \quad t > 0, \tag{3}$$

with the collision integral

$$\begin{aligned} Q(f)(\varepsilon) = C \int_{\mathbb{R}^3_+} \delta(\varepsilon + \varepsilon_* - \varepsilon' - \varepsilon'_*) S(\varepsilon, \varepsilon_*, \varepsilon', \varepsilon'_*)[f' f'_* (1+f)(1+f_*) \\ - f f_* (1+f')(1+f'_*)]\, d\varepsilon_* d\varepsilon' d\varepsilon'_*, \end{aligned} \tag{4}$$

where $C = m/(\pi^2\hbar^3)$ and $S \geq 0$ is a given function. Here $\hbar$ is the Planck constant and m denotes the mass of a particle. In the sequel we assume the equation has been normalized so that $C = 1$.

We denoted the density of states by

$$\rho(\varepsilon) = \int_{\mathbb{R}^6} \delta\left(\varepsilon - \left(\frac{|\mathbf{p}|^2}{2} + V(\mathbf{x})\right)\right) d\mathbf{p}\, d\mathbf{x}, \tag{5}$$

and

$$f' = f(\varepsilon', t), \quad f'_* = f(\varepsilon'_*, t), \quad f = f(\varepsilon, t), \quad f_* = f(\varepsilon_*, t). \tag{6}$$

As usual ε and ε_* are the pre-collisional energies of two interacting bosons and ε' and ε'_* are the post-collisional ones.

The positive measure

$$\delta(\varepsilon + \varepsilon_* - \varepsilon' - \varepsilon'_*) S(\varepsilon, \varepsilon_*, \varepsilon', \varepsilon'_*) \tag{7}$$

denotes the energy transition rate, i.e. $S d\varepsilon'\, d\varepsilon'_*$ is the transition probability per unit volume and per unit time that two bosons with incoming energies ε, ε_* are scattered with outgoing energies ε', ε'_*.

We remind that the phase-space density $F = F(\mathbf{x}, \mathbf{p}, t)$ satisfies the momentum-position space Boltzmann equation

$$\frac{\partial F}{\partial t} + \mathbf{p} \cdot \nabla_{\mathbf{x}} F - \nabla_{\mathbf{x}} V(\mathbf{x}) \cdot \nabla_{\mathbf{p}} F = \tilde{Q}(F), \tag{8}$$

with the scattering integral

$$\tilde{Q}(F)(\mathbf{x}, \mathbf{p}) = \frac{Q(F)\left(|\mathbf{p}|^2/2 + V(\mathbf{x})\right)}{\rho\left(|\mathbf{p}|^2/2 + V(\mathbf{x})\right)}. \tag{9}$$

In the homogeneous case $V(\mathbf{x}) \equiv 0$, F independent of $\mathbf{x}$, we set

$$\rho(\varepsilon) = \int_{\mathbb{R}^3} \delta\left(\varepsilon - \frac{|\mathbf{p}|^2}{2}\right) d\mathbf{p} \tag{10}$$

and compute

$$\rho(\varepsilon) = 4\pi\sqrt{2\varepsilon} \tag{11}$$

then equation (8) is formally identical to the Boson Boltzmann equation considered in [23],[24]

$$\begin{aligned}\frac{\partial F}{\partial t} = &\int_{\mathbb{R}^9} \delta(\mathbf{p}+\mathbf{p}_*-\mathbf{p}'-\mathbf{p}'_*)\delta(\varepsilon+\varepsilon_*-\varepsilon'-\varepsilon'_*)W(\mathbf{p},\mathbf{p}_*,\mathbf{p}',\mathbf{p}'_*)\\ &[F'F'_*(1+F)(1+F_*) - FF_*(1+F')(1+F'_*)]\, d\mathbf{p}_* d\mathbf{p}' d\mathbf{p}'_*,\end{aligned} \tag{12}$$

with $\varepsilon(\mathbf{p}) = |\mathbf{p}|^2/2$ and W, S are related by

$$\begin{aligned}&\int_{S^2\times S^2\times S^2} \delta(\mathbf{p}+\mathbf{p}_*-\mathbf{p}'-\mathbf{p}'_*)W(\mathbf{p},\mathbf{p}_*,\mathbf{p}',\mathbf{p}'_*)\, d\sigma_* d\sigma' d\sigma'_*\\ &= \frac{S\left(|\mathbf{p}|^2/2, |\mathbf{p}_*|^2/2, |\mathbf{p}'|^2/2, |\mathbf{p}'_*|^2/2\right)}{\rho(|\mathbf{p}|^2/2)\ |\mathbf{p}_*|\ |\mathbf{p}'|\ |\mathbf{p}'_*|}.\end{aligned}$$

Here we denoted $\mathbf{p}_* = |\mathbf{p}_*|\sigma_*$, $\mathbf{p}' = |\mathbf{p}'|\sigma'$, $\mathbf{p} = |\mathbf{p}|\sigma$, and $\mathbf{p}'_* = |\mathbf{p}'_*|\sigma'_*$. In particular for $W \equiv 1$ we have

$$S(\varepsilon, \varepsilon_*, \varepsilon', \varepsilon'_*) = \sigma\, \rho(\varepsilon_{\min}), \tag{13}$$

where (see [23])

$$\varepsilon_{\min} = \min(\varepsilon, \varepsilon_*, \varepsilon', \varepsilon'_*), \tag{14}$$

and σ is the total scattering cross section. We assume σ to be constant which is true for sufficiently small temperatures (where $\sigma \approx a_s^2$ and a_s is the wave scattering length[48]). Even in the non-homogeneous case $V(\mathbf{x}) \neq 0$ the equation (3) is formally identical to the isotropic version of the homogeneous bosonic Boltzmann equation (12) (after the introduction of $|\mathbf{p}|^2/2$ as new independent variable). However, the density of states is computed by formula (5) in the non homogeneous case instead of (10) in the space homogeneous case.

The above arguments remain valid in the case of a gas of fermions, that is quantum particles with half integer spin for which, by the Pauli exclusion principle, we have at most one particles on each orbital (electrons, protons, neutrons, ...) in contrast to bosons that have integer spin and for which the number of particles in a given state is arbitrary (carrier particles, mesons, ...). For a gas of fermions the QBE has the same structure except for the sign "-" instead of "+" and the collision operator reads

$$\begin{aligned}Q(f)(\varepsilon) = &\int_{\mathbb{R}^3_+} \delta(\varepsilon+\varepsilon_*-\varepsilon'-\varepsilon'_*)S(\varepsilon,\varepsilon_*,\varepsilon',\varepsilon'_*)[f'f'_*(1-f)(1-f_*)\\ &- ff_*(1-f')(1-f'_*)]\, d\varepsilon_* d\varepsilon' d\varepsilon'_*.\end{aligned} \tag{15}$$

2.2 Physical properties

A simple calculation gives the weak form of the collision operator. Let $\phi = \phi(\varepsilon)$ be a test function. Then, at least formally

$$\int_0^\infty Q(f)\phi d\varepsilon = \frac{1}{2}\int_{\mathbb{R}_+^4} \delta(\varepsilon+\varepsilon_*-\varepsilon'-\varepsilon'_*)S(\varepsilon,\varepsilon_*,\varepsilon',\varepsilon'_*)[f'f'_*(1+f)(1+f_*) - ff_*(1+f')(1+f'_*)][\phi+\phi_*-\phi'-\phi'_*]d\varepsilon d\varepsilon_* d\varepsilon' d\varepsilon'_*. \tag{16}$$

Here we used the micro-reversibility property, i.e. the fact that each collision is reversible and that each pair of interacting bosons represents a closed physical system. Mathematically this amounts to the requirement [23]

$$S(\varepsilon,\varepsilon_*,\varepsilon',\varepsilon'_*) = S(\varepsilon_*,\varepsilon,\varepsilon',\varepsilon'_*) = S(\varepsilon',\varepsilon'_*,\varepsilon,\varepsilon_*). \tag{17}$$

The symmetry properties (17) immediately imply the analogous properties for the energy transition rate (7) and the weak form (16) follows from the variable substitution in the integral using these symmetries.

As a consequence we have the following collision invariants

1.
$$\phi(\varepsilon) \equiv 1 \quad \Rightarrow \quad \int_0^\infty Q(f)(\varepsilon)\, d\varepsilon = 0, \tag{18}$$

2.
$$\phi(\varepsilon) \equiv \varepsilon \quad \Rightarrow \quad \int_0^\infty Q(f)(\varepsilon)\varepsilon\, d\varepsilon = 0. \tag{19}$$

Consider now the IVP (3) supplemented by the initial condition

$$f(\varepsilon, t=0) = f_0(\varepsilon) \geq 0, \quad \varepsilon > 0. \tag{20}$$

Then (18) implies mass conservation

$$\int_0^\infty \rho(\varepsilon) f(\varepsilon,t)\, d\varepsilon = \int_0^\infty \rho(\varepsilon) f_0(\varepsilon)\, d\varepsilon, \quad \forall\, t > 0, \tag{21}$$

and (19) energy conservation

$$\int_0^\infty \rho(\varepsilon) f(\varepsilon,t)\varepsilon\, d\varepsilon = \int_0^\infty \rho(\varepsilon) f_0(\varepsilon)\varepsilon\, d\varepsilon, \quad \forall\, t > 0. \tag{22}$$

The H-theorem for (3) is derived by setting $\phi(\varepsilon) = \ln(1+f(\varepsilon)) - \ln f(\varepsilon)$ in (16).

We calculate

$$\int_0^\infty Q(f)(\varepsilon)(\ln(1+f(\varepsilon)) - \ln f(\varepsilon))d\varepsilon = \frac{1}{2}\int_{\mathbb{R}_+^4} \delta(\varepsilon+\varepsilon_*-\varepsilon'-\varepsilon'_*)S(\varepsilon,\varepsilon_*,\varepsilon',\varepsilon'_*)e(f)d\varepsilon d\varepsilon_* d\varepsilon' d\varepsilon'_* := D[f], \tag{23}$$

where

$$e(f) = z(ff_*(1+f')(1+f'_*), f'f'_*(1+f)(1+f_*)) \tag{24}$$

and

$$z(x,y) = (x-y)(\ln x - \ln y). \tag{25}$$

Since the integrand of the entropy dissipation $D[f]$ is non-negative, we deduce the following H-theorem, obtained by multiplying (3) by $\phi(\varepsilon) = \ln(1+f(\varepsilon)) - \ln f(\varepsilon)$

$$\frac{d}{dt}S[f] = D[f], \tag{26}$$

which implies that the entropy

$$S[f] := \int_0^\infty \rho(\varepsilon)((1+f)\ln(1+f) - f\ln f)d\varepsilon, \tag{27}$$

is increasing along trajectories of (3). We remark that trivially the third physical conservation law, namely momentum conservation, also holds. Clearly the phase-space density F of (2) satisfies

$$\int_{\mathbb{R}^3} \mathbf{p}F(\mathbf{x},\mathbf{p},t)d\mathbf{x} \equiv 0, \quad \forall t \geq 0. \tag{28}$$

2.3 Steady states

We now turn to the issue of steady states of the QBE.

The main qualitative characteristics of f are described by these two properties: conservations and increasing entropy. It is therefore natural to expect that as t tends to ∞ the function f converges to a function f_∞ which realizes the maximum of the entropy $S[f]$ under the moments constraint (19)-(18). Clearly if f_∞ solves the entropy maximization problem with constraints (19)-(18), there exist Lagrange multipliers $\alpha, \beta \in \mathbb{R}$ such that

$$\int \rho(\varepsilon)(\ln(1+f_\infty(\varepsilon)) - \ln f_\infty(\varepsilon))\phi(\varepsilon)\,d\varepsilon = \int \rho(\varepsilon)(\alpha\varepsilon+\beta)\phi(\varepsilon)\,d\varepsilon, \qquad \forall\,\phi \tag{29}$$

which implies

$$\ln(1+f_\infty(\varepsilon)) - \ln f_\infty(\varepsilon) = \alpha\varepsilon + \beta$$

and therefore

$$f_\infty(\varepsilon) = \frac{1}{e^{\alpha\varepsilon+\beta}-1}, \quad \alpha > 0, \beta \in \mathbb{R}. \tag{30}$$

The function f_∞ is called a Bose-Einstein distribution. Again if we consider a gas of of fermions the only difference results in the sign and reads

$$f_\infty(\varepsilon) = \frac{1}{e^{\alpha\varepsilon+\beta}+1}, \quad \alpha > 0, \beta \in \mathbb{R} \tag{31}$$

called a Fermi-Dirac distribution (see [23] for more detalis).

The problem of equilibrium distributions for bosons has a very long history, going back to Bose and Einstein in the twenties of the last century (see [11],[19],[20]), who noticed that the class of Bose-Einstein distributions (30) is not sufficient to assume all possible values of equilibrium mass

$$M_\infty = \int_0^\infty \rho(\varepsilon) f_\infty(\varepsilon) d\varepsilon, \tag{32}$$

and equilibrium energy

$$E_\infty = \int_0^\infty \rho(\varepsilon)\varepsilon f_\infty(\varepsilon) d\varepsilon, \tag{33}$$

such that Dirac distribution have to be included in the set of equilibrium states. In [23] it was shown that for every pair $(M_\infty, E_\infty) \in \mathbb{R}^2_+$ there exist $\alpha \geq 0$, $\beta \in \mathbb{R}$ such that the generalized Bose-Einstein distribution defined by

$$\rho(\varepsilon) f_\infty(\varepsilon) = \frac{\rho(\varepsilon)}{e^{\alpha\varepsilon+\beta_+} - 1} + |\beta_-|\delta(\varepsilon), \tag{34}$$

is an equilibrium state of (3) satisfying (32)-(33). Here we denoted $\beta_+ = \max(\beta, 0)$ and $\beta_- = -\max(-\beta, 0)$. The value $M_{\infty,cond} = |\beta_-|$ represents the mass-fraction of particles which are condensed in equilibrium, i.e. in their quantum mechanical ground state with $\varepsilon = 0$.

In the following sections we shall use

$$S(\varepsilon, \varepsilon_*, \varepsilon', \varepsilon'_*) = \rho(\varepsilon_{\min}). \tag{35}$$

Notice that the condensation is fully localized in phase space, i.e. it may only occur at $p = 0$ (vanishing momentum) and at those points in position space, where the potential assumes its minimum value 0. The reason for this is the form (2) of the phase space distribution and a semiclassical limit process which leads to the Boson Boltzmann equation (3).

3 Numerical methods

We consider the IVP for the quantum Boltzmann equation

$$\rho(\varepsilon)\frac{\partial f}{\partial t} = Q(f)(\varepsilon), \quad t > 0, \tag{36}$$

$$f(\varepsilon, t = 0) = f_0(\varepsilon) \geq 0. \tag{37}$$

Here the independent variable $\varepsilon > 0$ represents the kinetic energy, $\rho = \rho(\varepsilon) \geq 0$ is the (given) density of states and the boson collision operator now reads

$$\begin{aligned} Q(f)(\varepsilon) = \int_{\mathbb{R}^3_+} \delta(\varepsilon + \varepsilon_* - \varepsilon' - \varepsilon'_*)\rho(\varepsilon_{\min})[f' f'_*(1+f)(1+f_*) \\ - f f_*(1+f')(1+f'_*)]\, d\varepsilon_* d\varepsilon' d\varepsilon'_*. \end{aligned} \tag{38}$$

Obviously the equation (36) maintains a minimum principle such that solution of (36), (37) satisfy $f(\varepsilon,t)\geq 0$ for $\varepsilon\geq 0, t>0$ if $f_0(\varepsilon)\geq 0$ for $\varepsilon>0$. Although our treatment will be restricted to the case of of bosons it can be applied straightforwardly to the case of fermions.

3.1 Discretization and main properties

The starting point in the development of a numerical scheme for (38) is the definition of a bounded domain approximation of the collision operator Q.

Let f be defined for $\varepsilon\in[0,R]$ and denote

$$\begin{aligned} Q_R(f)(\varepsilon) = \int_{[0,R]^3} \delta(\varepsilon+\varepsilon_*-\varepsilon'-\varepsilon'_*)\rho(\varepsilon_{\min})[f'f'_*(1+f)(1+f_*) \\ - ff_*(1+f')(1+f'_*)]\psi(\varepsilon\leq R)\,d\varepsilon_* d\varepsilon' d\varepsilon'_* \end{aligned} \tag{39}$$

where $\psi(I)$ is the indicator function of the set I. Then, at least formally

$$\begin{aligned} \int_0^\infty Q_R(f)\phi d\varepsilon = \frac{1}{2}\int_{[0,R]^4} \delta(\varepsilon+\varepsilon_*-\varepsilon'-\varepsilon'_*)\rho(\varepsilon_{\min})[f'f'_*(1+f)(1+f_*) \\ - ff_*(1+f')(1+f'_*)][\phi+\phi_*-\phi'-\phi'_*]d\varepsilon d\varepsilon_* d\varepsilon' d\varepsilon'_* \end{aligned} \tag{40}$$

for any test function $\phi=\phi(\varepsilon)$. The proof follows the lines of the corresponding weak form of Q discussed in Section 2. It is easy to check that the weak formulation (40) of Q_R implies mass and energy conservation as well as entropy inequality over the bounded domain.

Let us now introduce a set of equally spaced discrete energy grid points $\varepsilon_1\leq\varepsilon_2\leq\ldots\leq\varepsilon_N$ in $[0,R]$. We will restrict to product quadrature rules with equal weights $w=R/N$ such that

$$\int_0^R f(\varepsilon)\,d\varepsilon \approx w\sum_{i=1}^N f(\varepsilon_i).$$

A general quadrature formula for (39) is given by

$$\begin{aligned} Q_R(f)(\varepsilon_i)\approx \tilde{Q}_R(f)(\varepsilon_i) = w^3\sum_{j,k,l=1}^N \delta_{ij}^{kl}\,\rho(\varepsilon_{\min})[f_kf_l(1+f_i)(1+f_j) \\ - f_if_j(1+f_k)(1+f_l)]\psi(\varepsilon_i\leq R), \end{aligned} \tag{41}$$

where now $f_i=f(\varepsilon_i)$ and $\varepsilon_{\min}=\min\{\varepsilon_i,\varepsilon_j,\varepsilon_k,\varepsilon_l\}$. The quantities δ_{ij}^{kl} are suitable discretization of the δ-function on the grid.

In order to maintain the conservation properties on the discrete level it is of paramount importance that the discretized δ-function will reduce the points in the sum to a discrete index set which satisfies the relation $i + j = k + l$.

We now consider the set of ODEs which originates from the energy discretization of the IVP for Q_R

$$\rho(\varepsilon_i)\frac{df_i}{dt} = \tilde{Q}_R(f)(\varepsilon_i), \quad t > 0, \tag{42}$$

$$f_i(t=0) = f_{0,R}(\varepsilon_i) \geq 0. \tag{43}$$

and state [40]

Proposition 1. *If we define*

$$\delta_{ij}^{kl} = \begin{cases} 1/w \; i+j=k+l \\ 0 \quad \text{otherwise} \end{cases} \tag{44}$$

the solutions of the IVP (42), (43) satisfy the following discrete conservation properties and entropy principle

$$w\sum_{i=1}^{N}\rho(\varepsilon_i)\frac{df_i}{dt}\phi(\varepsilon_i) = 0, \qquad \phi(\varepsilon) = 1, \quad \phi(\varepsilon) = \varepsilon, \tag{45}$$

$$w\sum_{i=1}^{N}\rho(\varepsilon_i)\frac{dh(f_i)}{dt} \geq 0, \qquad h(f_i) = (1+f_i)\log(1+f_i) - f_i\log f_i. \tag{46}$$

Due to the definition of δ_{ij}^{kl} we have the quadrature formula

$$\begin{aligned}\tilde{Q}_R(f)(\varepsilon_i) = w^2 \sum_{\substack{j,l=1 \\ 1\leq k=i+j-l\leq N}}^{N} \rho(\varepsilon_{\min})[f_k f_l(1+f_i)(1+f_j) \\ - f_i f_j(1+f_k)(1+f_l)].\end{aligned} \tag{47}$$

It is easy to check by direct verification [40] that these schemes admits discrete Bose-Einstein equilibrium states of the form

$$f_\infty(\varepsilon_i) = \frac{1}{e^{\alpha\varepsilon_i+\beta}-1}, \quad \alpha > 0, \beta \in \mathbb{R}. \tag{48}$$

More delicate is the question of 'generalized' discrete Bose-Einstein equilibrium which will be discussed later on.

3.2 First and second order methods

Let us rewrite for $\varepsilon \in [0, R]$ the collision integral (39) as

$$Q_R(f)(\varepsilon) = \int_0^R \int_{S(\varepsilon,\varepsilon')}^{D(\varepsilon,\varepsilon')} \rho(\varepsilon_{\min}) F(\varepsilon, \varepsilon', \varepsilon'_*)\, d\varepsilon'_* d\varepsilon', \tag{49}$$

where $F(\varepsilon, \varepsilon', \varepsilon'_*) = [f' f'_* (1+f)(1+f_*) - f f_* (1+f')(1+f'_*)]$, with $\varepsilon_* = \varepsilon' + \varepsilon'_* - \varepsilon$, and $S(\varepsilon, \varepsilon') = \max\{\varepsilon - \varepsilon', 0\}$, $D(\varepsilon, \varepsilon') = \min\{\varepsilon - \varepsilon' + R, R\}$. The integration domain for a fixed value of ε in the $(\varepsilon', \varepsilon'_*)$ plane is shown in figure 1.

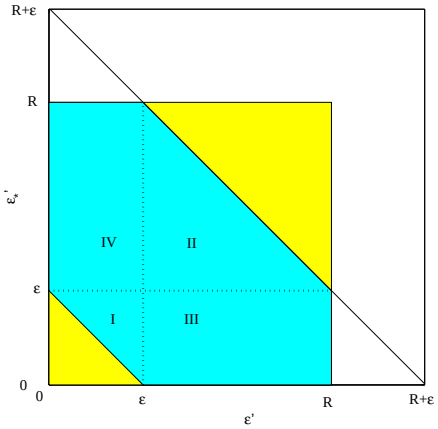

Fig. 1. The computational domain (dark gray region) in the (ϵ', ϵ'_*) plane for a fixed ε

We need the following [40]

Lemma 1. *We have*

$$\rho(\varepsilon_{\min}) = \begin{cases} \rho(\varepsilon_*) & (\varepsilon', \varepsilon'_*) \in \mathrm{I} \\ \rho(\varepsilon) & (\varepsilon', \varepsilon'_*) \in \mathrm{II} \\ \rho(\varepsilon'_*) & (\varepsilon', \varepsilon'_*) \in \mathrm{III} \\ \rho(\varepsilon') & (\varepsilon', \varepsilon'_*) \in \mathrm{IV} \end{cases} \tag{50}$$

where the regions I, II, III, IV represent a partition of the computational domain and are shown in figure 1.

Using the previous lemma the integral (49) over the four regions can be decomposed as

$$Q_R(f)(\varepsilon) = I_1(\varepsilon) + I_2(\varepsilon) + I_3(\varepsilon) + I_4(\varepsilon), \tag{51}$$

where for example we have

$$I_1(\varepsilon) = \int_0^{\varepsilon} \int_{\varepsilon - \varepsilon'}^{\varepsilon} \rho(\varepsilon' + \varepsilon'_* - \varepsilon) F(\varepsilon, \varepsilon', \varepsilon'_*)\, d\varepsilon'_* d\varepsilon', \tag{52}$$

and similarly for the other regions.

In the same way the quadrature formula (47) can be decomposed as

$$\tilde{Q}_R(f)(\varepsilon_i) = \tilde{I}_1(\varepsilon_i) + \tilde{I}_2(\varepsilon_i) + \tilde{I}_3(\varepsilon_i) + \tilde{I}_4(\varepsilon_i), \tag{53}$$

where now

$$\tilde{I}_1(\varepsilon_i) = w^2 \sum_{k=1}^{i} \sum_{l=i-k+1}^{i} \rho(\varepsilon_k + \varepsilon_l - \varepsilon_i) F(\varepsilon_i, \varepsilon_k, \varepsilon_l). \tag{54}$$

From the point of view of accuracy we can state [40]

Theorem 1 (Consistency). *Let the function f and ρ be $C^m([0,R])$, $m = 1$ or $m = 2$, then the quadrature formula (47) satisfies*

$$|Q_R(f)(\varepsilon_i) - \tilde{Q}_R(f)(\varepsilon_i)| \le R^2 C_m (\Delta\varepsilon)^m M_m, \qquad \Delta\varepsilon = R/N, \tag{55}$$

where M_m is a constant that depends on f and ρ and their derivatives up to the order m. Moreover if $\varepsilon_i = (i-1)\Delta\varepsilon$, $i = 1, \ldots, N$ (rectangular rule) *then $m = 1$ and $C_m = 1/2$, whereas if $\varepsilon_i = (i - 1/2)\Delta\varepsilon$, $i = 1, \ldots, N$* (midpoint rule) *$m = 2$ and $C_m = 1/24$.*

3.3 Fast algorithms

Finally we will analyze the problem of the computational cost of the quadrature formula (47). A straightforward analysis shows that the evaluation of the double sum in (47) at the point ε_i requires $(2(i-1)(N-i+1) + N^2)/2$ operations. The overall cost for all N points is then approximatively $2N^3/3$. However using transform techniques and the decomposition (53) this $O(N^3)$ cost can be reduced to $O(N^2 \log_2 N)$.

In order to do this let us set $h = k + l = i + j$ in (47) and rewrite

$$\begin{aligned} \tilde{Q}_R(\varepsilon_i) = w^2 \sum_{h=2}^{2N} \sum_{k=1}^{N} \rho(\varepsilon_{\min}) [& f_k f_{h-k} (1+f_i)(1+f_{h-i}) \\ & - f_i f_{h-i} (1+f_k)(1+f_{h-k})] \Psi_{h-i}^{[1,N]} \Psi_{h-k}^{[1,N]}, \end{aligned} \tag{56}$$

where we have set

$$\Psi_i^{[s,d]} = \begin{cases} 1 & s \le i \le d \\ 0 & \text{otherwise} \end{cases} \tag{57}$$

In (56) we assume that the function f_i is extended to $i = 1, \ldots, 2N$ by padding zeros for $i > N$.

The sum (56) can be split into sum over the four regions which characterize $\rho(\varepsilon_{\min})$. We shall give the details of the fast algorithm only for region I, the other regions can be treated similarly. We have

$$\tilde{I}_1(\varepsilon_i) = w^2 \sum_{h=2}^{2N} \sum_{k=1}^{i} \rho(\varepsilon_{h-i})[f_k f_{h-k}(1+f_i)(1+f_{h-i}) - f_i f_{h-i}(1+f_k)(1+f_{h-k})]\Psi_{h-i}^{[1,i]}\Psi_{h-k}^{[1,i]}, \tag{58}$$

or equivalently

$$\tilde{I}_1(\varepsilon_i) = w^2 \sum_{h=2}^{2N} \rho(\varepsilon_{h-i})(1+f_i)(1+f_{h-i})\Psi_{h-i}^{[1,i]} S_h^1(i) - w^2 \sum_{h=2}^{2N} \rho(\varepsilon_{h-i}) f_i f_{h-i} \Psi_{h-i}^{[1,i]} S_h^2(i),$$

where we have set

$$S_h^1(i) = \sum_{k=1}^{i} f_k f_{h-k} \Psi_{h-k}^{[1,i]}, \quad S_h^2(i) = \sum_{k=1}^{i} (1+f_k)(1+f_{h-k})\Psi_{h-k}^{[1,i]}. \tag{59}$$

Now the two sums $S_h^1(i)$ and $S_h^2(i)$ are discrete convolutions and can be evaluated for all h and i using the FFT algorithm in $O(N^2 \log_2 N)$ operations [40].

Remark 1. In the case of constant ρ it is easy to show that expression (56) reduces to a double convolution sum which can be evaluated using the FFT in only $O(N \log_2 N)$ operations instead of $O(N^2 \log_2 N)$.

3.4 Numerical examples

In this section we present some numerical examples, we refer the reader to [40] for further numerical results. We shall refer to the first and second order fast schemes developed in the previous section by *QBF1* and *QBF2* respectively. The time integration is performed with standard first and second order explicit Runge-Kutta schemes after dividing equation (42) by $\rho(\varepsilon_i)$ and thus rewriting the semidiscrete schemes as

$$\frac{\partial f_i}{\partial t} = w^2 \sum_{\substack{j,l=1 \\ 1 \le k = i+j-l \le N}}^{N} \frac{\rho(\varepsilon_{\min})}{\rho(\varepsilon_i)} [f_k f_l (1+f_i)(1+f_j) - f_i f_j (1+f_k)(1+f_l)]. \tag{60}$$

In all our numerical tests the density of states is given by

$$\rho(\varepsilon) = \frac{\varepsilon^2}{2}, \tag{61}$$

which corresponds to an harmonic potential $V(x)$.

Note that $0 \leq \rho(\varepsilon_{\min})/\rho(\varepsilon_i) \leq 1$ for $\varepsilon_i \neq 0$ and that as $\varepsilon_i \to 0$ we have $\rho(\varepsilon_{\min})/\rho(\varepsilon_i) \to 1$. Furthermore since $\rho(0) = 0$ the values of the distribution function at $\varepsilon_i = 0$ does not affect the discrete conservation of mass and energy.

The schemes were implemented using the fast algorithm described in Section 3.3.

Bose-Einstein equilibrium

The initial datum is a Gaussian profile centered at $R/2$

$$f = \exp(-4(\varepsilon - R/2)^2), \tag{62}$$

with $R = 10$. We compute the large time behavior of the schemes for $N = 40$. The stationary solution at $t = 10$ is given in Figure 2 for both schemes together with the numerically computed entropy growth. As observed the methods converge to the same stationary state given by a 'regular' discrete Bose-Einstein distribution.

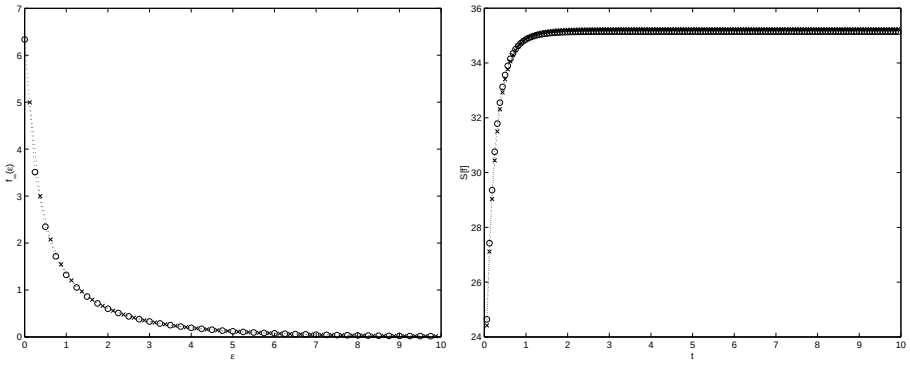

Fig. 2. Stationary discrete Bose-Einstein equilibrium and entropy growth for scheme QBF1 (∘) and QBF2 (×) computed with $N = 40$ points.

The trend to equilibrium in time for the two schemes is reported in Figures 3. Note that although the two schemes agree very well there is a remarkable resolution difference in proximity of the point $\varepsilon = 0$ due to the staggered grids of the schemes.

Condensation

In this test we consider the process of condensation of bosons. It is a fundamental results of quantum statistics of bosons that above a certain critical density particles enter the ground state, that is a Bose-Einstein condensate

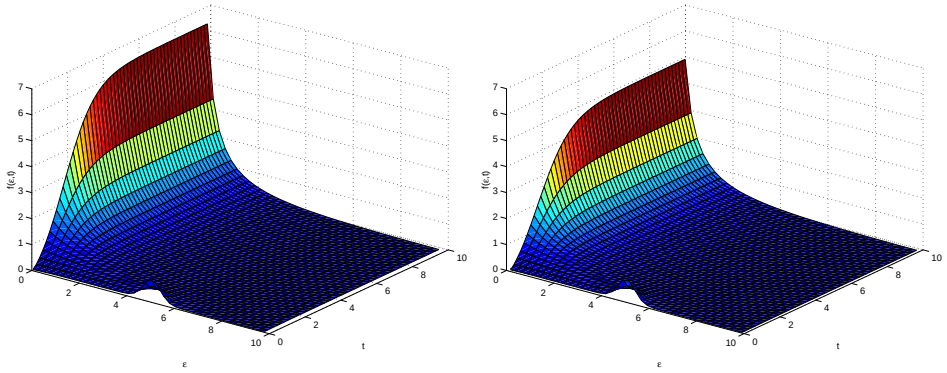

Fig. 3. Trend to equilibrium in time for scheme QBF1 (left) and QBF2 (right) computed with $N = 40$ points.

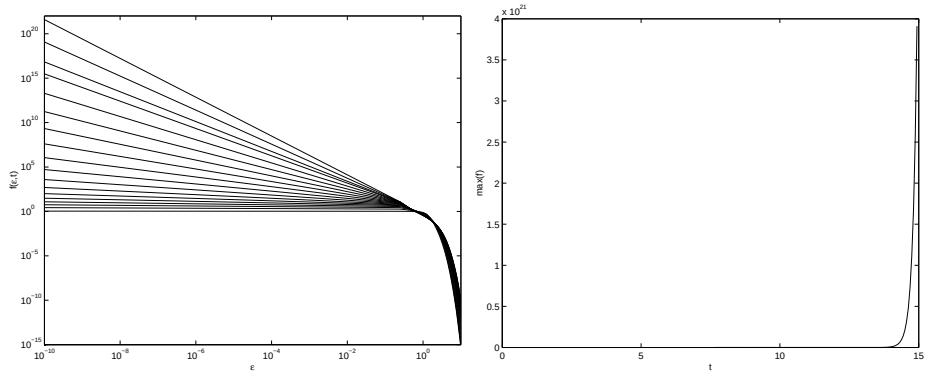

Fig. 4. Distribution of bosons at different times in logarithmic scale (left) and its maximum value (right) during condensation with scheme QBF1 with $N = 40$ points.

forms (see [26],[27],[25],[45],[46]) and the equilibrium distribution f_∞ is of the form (34) with $\beta_- \neq 0$.

Note that for the second order method, unlike the first order one, due to the midpoint quadrature, we have $\varepsilon_i \neq 0$ for all gridpoints. Thus we expect to get a better resolution of the singularity in $\varepsilon = 0$ with the first order scheme.

We choose the initial distribution in the energy interval $[0, R]$ with $R = 10$ to be[45],[46]

$$f(\epsilon) = \frac{2f_0}{\pi} \arctan(e^{\Gamma(1-\epsilon/\epsilon_0)}), \tag{63}$$

with $\Gamma = 5$ and $\epsilon_0 = R/8$. At values of f_0 larger than a critical f_0^* the formation of a condensate occurs (see [45],[46]). We choose $f_0 = 1$, which turns on to be supercritical and integrate the Boson Boltzmann equation up to $T = 15$. The results we obtain with the two schemes for $N = 40$ are

considerably different near the point $\varepsilon = 0$. The results for scheme QBF1 are reported in Figures 4.

A magnified view of the numerical solutions obtained with $N = 40$ and $N = 80$ points shows that away from the singularity the two schemes are still in good agreement (see Figure 5).

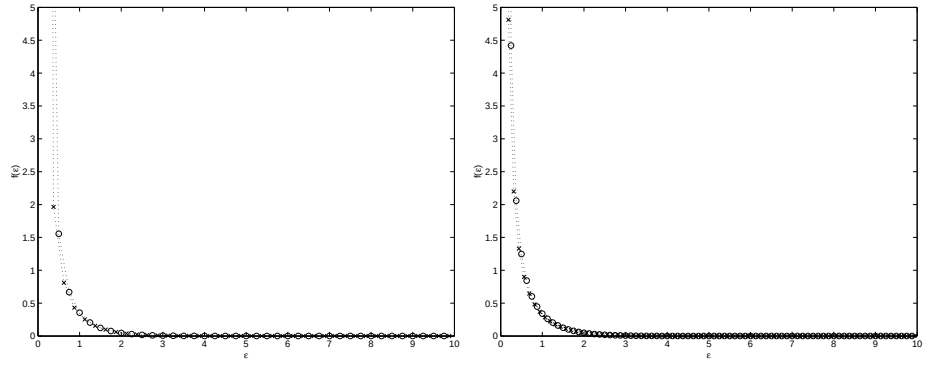

Fig. 5. Magnified view of the distribution of bosons at the final computation time during condensation with scheme QBF1 ($\circ$) and scheme QBF2 ($\times$) with $N = 40$ (left) and $N = 80$ (right) points.

4 Time dependent trapping potentials

In order to study the formation of Bose-Einstein condensate from an uncondensed harmonically trapped gas of bosons by changing the shape of the trapping potential we consider here the case of time dependent trapping potential [31]. In particular we will extend the above method to the case of an harmonic trap potential with a time dependent depth of the dip.

The analytic expression of the potential is

$$V(\mathbf{x}, t) = \frac{1}{2} m\omega_1^2 \mathbf{x}^2 + \left(\frac{1}{2} m\omega_2^2 \mathbf{x}^2 - U_0(t) \right) \theta(R(t) - |\mathbf{x}|) \tag{64}$$

where θ is the Heavyside step function, R is the radius of the narrow dip in the center of the trap and is given by

$$R(t) = \sqrt{2U_0(t)/m(\omega_1^2 - \omega_2^2)},$$

with

$$U_0(t) = U_0 \left(1 - \frac{2}{1 + \exp(t/t_s)} \right), \tag{65}$$

where t_s is a reference scaling time.

In the energy dependent case we have the following QBE in conservative form

$$\frac{\partial}{\partial t}(\rho(t,\varepsilon)f(t,\varepsilon)) + \frac{\partial}{\partial \varepsilon}(G(t,\varepsilon)f(t,\varepsilon)) = Q(f)(t,\varepsilon) \tag{66}$$

supplemented with the initial condition $f(0,\varepsilon) = f_0(\varepsilon)$. Equation (66) is considered in the time dependent domain $\epsilon \in \Omega(t) = [\varepsilon_0(t), \infty[$ with $\varepsilon_0(t) = -U_0(t)$. The density of states $\rho(t,\varepsilon)$ and the function $G(t,\varepsilon)$ are given by

$$\rho(t,\varepsilon) = \frac{2\pi(2m)^{3/2}}{(2\pi\hbar)^3} \int_{V(\mathbf{x},t)<\varepsilon} \sqrt{\varepsilon - V(\mathbf{x},t)}\, d\mathbf{x}, \tag{67}$$

$$G(t,\varepsilon) = \frac{2\pi(2m)^{3/2}}{(2\pi\hbar)^3} \int_{V(\mathbf{x},t)<\varepsilon} \frac{\partial V(\mathbf{x},t)}{\partial t} \sqrt{\varepsilon - V(\mathbf{x},t)}\, d\mathbf{x}. \tag{68}$$

We assume $\kappa = (\omega_1/\omega_2)^3 \ll 1$ and find the approximate expressions [31]

$$\rho(t,\varepsilon) = \frac{(\varepsilon + U_0(t))^2}{2(\hbar\omega_2)^3}\theta(\varepsilon + U_0(t)) + \frac{\varepsilon^2}{2(\hbar\omega_1)^3} \tag{69}$$

$$G(t,\varepsilon) = -\dot{U_0}(t)\frac{(\varepsilon + U_0(t))^2}{2(\hbar\omega_2)^3}\theta(\varepsilon + U_0(t)). \tag{70}$$

We recall that

$$\begin{aligned} Q(f)(t,\varepsilon) = C\sigma \int_{\Omega(t)^3} d\varepsilon_1\, d\varepsilon_2\, d\varepsilon_3\, \delta(\varepsilon_1 + \varepsilon_2 - \varepsilon_3 - \varepsilon)\rho(t,\varepsilon_{\min}) \\ [f_1 f_2(1+f_3)(1+f) - f_3 f(1+f_1)(1+f_2)] \end{aligned} \tag{71}$$

with $\varepsilon_{\min} = \min(\varepsilon_1, \varepsilon_2, \varepsilon_3, \varepsilon)$, $f_i = f(t,\varepsilon_i)$ and $C = m/(\pi^2\hbar^3)$.

4.1 The numerical method

In order to solve numerically equation (66) it is convenient to introduce the change of variables $\tilde{\epsilon} = \varepsilon + U_0(t)$ and use the notations

$$\tilde{f}(t,\tilde{\epsilon}) = f(t,\tilde{\epsilon} - U_0(t)), \quad \tilde{\rho}(t,\tilde{\epsilon}) = \rho(t,\tilde{\epsilon} - U_0(t)), \quad \tilde{G}(t,\tilde{\epsilon}) = G(t,\tilde{\epsilon} - U_0(t)).$$

From (66) since

$$\frac{\partial}{\partial t}(\rho(t,\varepsilon)f(t,\varepsilon)) = \frac{\partial}{\partial t}(\tilde{\rho}(t,\tilde{\epsilon})\tilde{f}(t,\tilde{\epsilon})) + \dot{U_0}(t)\frac{\partial}{\partial \tilde{\epsilon}}(\tilde{\rho}(t,\tilde{\epsilon})\tilde{f}(t,\tilde{\epsilon})),$$

we get

$$\frac{\partial}{\partial t}(\tilde{\rho}(t,\tilde{\epsilon})\tilde{f}(t,\tilde{\epsilon})) + \frac{\partial}{\partial \tilde{\epsilon}}((\tilde{\rho}(t,\tilde{\epsilon})\dot{U_0}(t) + \tilde{G}(t,\tilde{\epsilon}))\tilde{f}(t,\tilde{\epsilon})) = \tilde{Q}(\tilde{f})(t,\tilde{\epsilon}) \tag{72}$$

where now $\tilde{\epsilon} \in \mathbb{R}^+$ and

$$\tilde{Q}(\tilde{f})(t,\tilde{\epsilon}) = C \int_{(\mathbb{R}^+)^3} d\tilde{\epsilon}_1\, d\tilde{\epsilon}_2\, d\tilde{\epsilon}_3\, \delta(\tilde{\epsilon}_1 + \tilde{\epsilon}_2 - \tilde{\epsilon}_3 - \tilde{\epsilon})\tilde{\rho}(t,\tilde{\epsilon}_{\min}) \\ [\tilde{f}_1\tilde{f}_2(1+\tilde{f}_3)(1+\tilde{f}) - \tilde{f}_3\tilde{f}(1+\tilde{f}_1)(1+\tilde{f}_2)]. \tag{73}$$

Problem (72) is considered with the initial condition $\tilde{f}(0,\tilde{\epsilon}) = f_0(\tilde{\epsilon}) = f_0(\varepsilon)$.

The numerical solution to (72) is carried out on a finite energy range $\tilde{\epsilon} \in [0,R]$ with $R > 0$. Clearly the choice of R should be done carefully so that the error on the density function f due to the finite energy range is negligible.

The discretization of the collision operator $\tilde{Q}(\tilde{f})$ in (73) is done with the methods presented before.

Note that from (14) and (15)

$$\tilde{\rho}(t,\tilde{\epsilon})\dot{U}_0(t) + \tilde{G}(t,\tilde{\epsilon}) = \dot{U}_0(t)\frac{(\tilde{\epsilon} - U_0(t))^2}{2(\hbar\omega_1)^3}\theta(\tilde{\epsilon} - U_0(t)) \geq 0.$$

In particular from (7) we have that (72) can be written as

$$\tilde{\rho}(t,\tilde{\epsilon})\frac{\partial}{\partial t}\tilde{f}(t,\tilde{\epsilon}) + (\tilde{\rho}(t,\tilde{\epsilon})\dot{U}_0(t) + \tilde{G}(t,\tilde{\epsilon}))\frac{\partial}{\partial \tilde{\epsilon}}\tilde{f}(t,\tilde{\epsilon}) = \tilde{Q}(\tilde{f}), \tag{74}$$

which describes a transport of the density function f with a nonnegative characteristic speed

$$z(t,\tilde{\epsilon}) = \begin{cases} \dfrac{\tilde{\rho}(t,\tilde{\epsilon})\dot{U}_0(t) + \tilde{G}(t,\tilde{\epsilon})}{\tilde{\rho}(t,\tilde{\epsilon})} & \tilde{\epsilon} > U_0(t) \\ \\ 0 & \tilde{\epsilon} \leq U_0(t), \end{cases} \tag{75}$$

since $\lim_{\tilde{\epsilon}\to 0} \tilde{G}(t,\tilde{\epsilon})/\tilde{\rho}(t,\tilde{\epsilon}) = -\dot{U}_0(t)$. Thus no boundary condition is needed on the computational domain $[0,R]$. The advection part in (74) has been solved with a third order method along characteristics using equation (20).

For the time discretization we used a second order Strang[47] splitting method. The collision part in (74) is solved with a second order explicit Runge-Kutta scheme. Thus the overall accuracy of our schemes will be second order both in time and energy variables. Moreover it can be shown that the resulting schemes preserves the nonnegativity of the solution under a suitable CFL condition that depends on $z(t,\varepsilon)$ and the function f.

4.2 Numerical results

We have computed the numerical solution of equation (72) for several test problems. The initial data is an equilibrium Bose-Einstein distribution with a given temperature $kT_0/\hbar\omega_1 = T$, a given chemical potential $\mu_0/\hbar\omega_1 = \mu$, a fixed trap frequency ratio of $\omega_2/\omega_1 = \kappa$. The constant $t_c = t_{\rm mfp}/10$ where $t_{\rm mfp} = 6.8 \times 10^{-4}$ is the mean free collision time at the center of the trap. All the numerical solutions have been obtained with $N = 100$ grid points and $C\sigma = 1$.

Test 1: ($U_0 < U_c$)

The data for this test are: $T = 475$, $\mu = -1465$, $U_0 = 1500$ and $R = 6000$. The solution has been computed at time $t = 0.004$ for $\kappa = 0.1, 0.01, 0.001$.

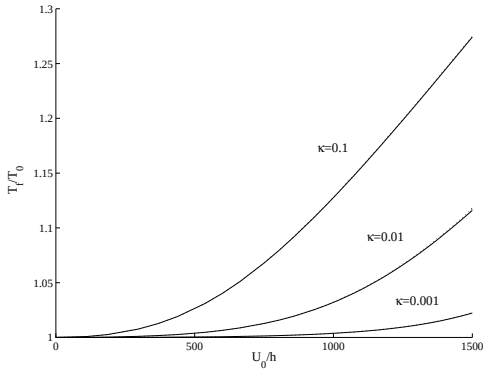

Fig. 6. Test 1. Temperature increase versus $U_0/\hbar$ in QBE (continuous line) and in the collisionless equation (dotted line) for various κ.

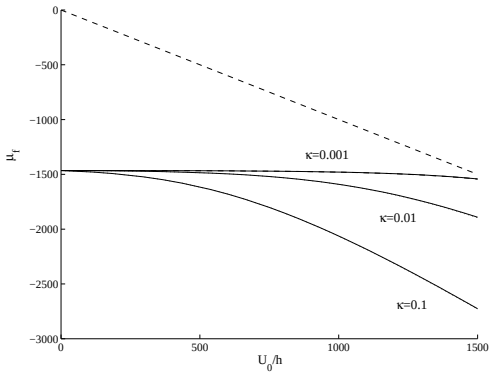

Fig. 7. Test 1. Chemical potential decrease versus U_0 in QBE continuous line) and in the collisionless equation (dotted line) for various κ. The dashed line corresponds to $-U(t)$. For $\kappa = 0.001$ the value $U_0 = -1500$ is almost critical.

In Figure 6 and 7 we report the temperature and the chemical potential profiles versus U_0 for various κ.

Test 2: ($U_0 > U_c \neq 0$)

The data for this test are: $T = 1000$, $\mu = -768$, $U_0 = 850$, $\kappa = 0.1, 0.01$ and $R = 10000$. The solution has been computed at time $t = 0.001$. For $\kappa = 0.01$ condensation is observed when $U(t) \geq 790$.

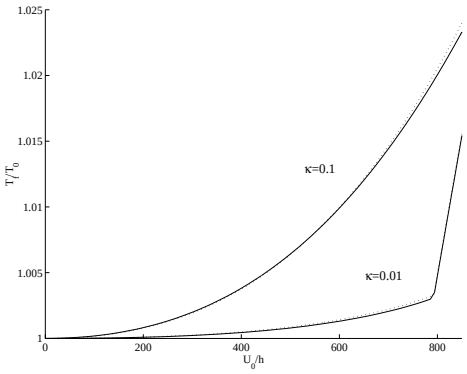

Fig. 8. Test 2. Temperature increase versus $U_0/\hbar$ in QBE (continuous line) and the collisionless equation (dotted line).

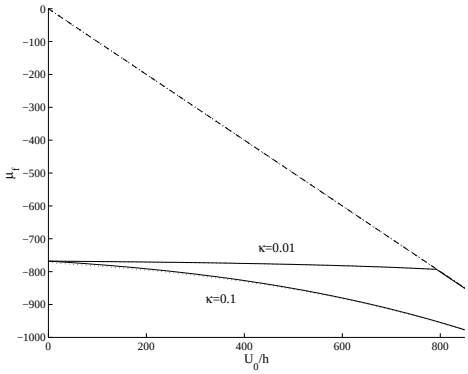

Fig. 9. Test 2. Chemical potential decrease versus $U_0/\hbar$ in QBE (continuous line) and the collisionless equation (dotted line). The dashed line corresponds to $-U(t)$.

In Figure 8, 9 and 10 we report the temperature, the chemical potential and the condensate profiles versus U_0.

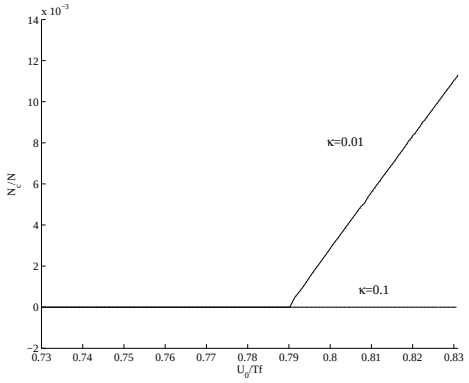

Fig. 10. Test 2. Fraction of condensate versus U_0/kT_f in QBE (continuous line) and the collisionless equation (dotted line). For $U(t) \geq 790$ condensation is observed.

Test 3: $(U_0 > U_c = 0)$

The data for this test are: $T = T_c$, $\mu = 0$, $U_0 = 400$, $\kappa = 0.2, 0.01$ and $R = 1500$. Numerically we have used a small tolerance $\tau = 0.0025U_0$ as initial value for μ to avoid the singularity at $\epsilon = 0$.

The solution has been computed at time $t = 0.0005$.

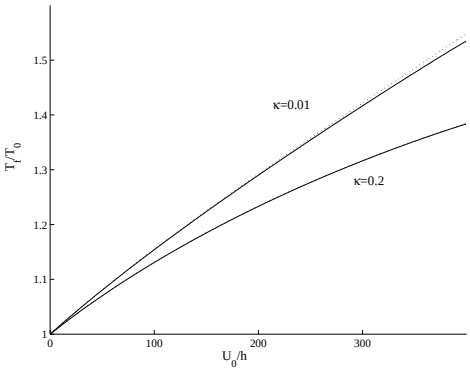

Fig. 11. Test 3. Temperature increase versus $U_0/\hbar$ in QBE. Dotted lines refer to collisionless result.

In Figure 11 and 12 we report the temperature and the condensate profiles versus U_0.

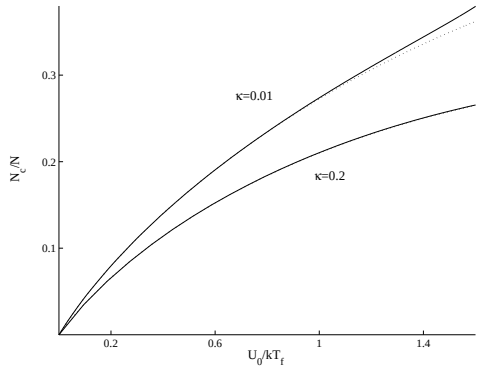

Fig. 12. Test 3. Fraction of condensate versus U_0/kT_f in QBE. Dotted lines refer to collisionless result.

5 The Gross-Pitaevskii equation

At temperatures T much smaller than the critical temperature T_c [34], a BEC is well described by the macroscopic wave function $\psi = \psi(\mathbf{x}, t)$ whose evolution is governed by a self-consistent, mean field nonlinear Schrödinger equation (NLSE) known as the Gross-Pitaevskii equation (GPE) [30, 44]

$$i\hbar\frac{\partial\psi(\mathbf{x},t)}{\partial t} = -\frac{\hbar^2}{2m}\nabla^2\psi(\mathbf{x},t) + V(\mathbf{x})\psi(\mathbf{x},t) + NU_0|\psi(\mathbf{x},t)|^2\psi(\mathbf{x},t), \quad (76)$$

where m is the atomic mass, $\hbar$ is the Planck constant, N is the number of atoms in the condensate, $V(\mathbf{x})$ is an external trapping potential. When a harmonic trap potential is considered, $V(\mathbf{x}) = \frac{m}{2}\left(\omega_x^2x^2 + \omega_y^2y^2 + \omega_z^2z^2\right)$ with ω_x, ω_y and ω_z being the trap frequencies in x, y and z-direction, respectively. For the following we assume (w.r.o.g.) $\omega_x \le \omega_y \le \omega_z$. $U_0 = 4\pi\hbar^2a_s/m$ describes the interaction between atoms in the condensate with a_s the s-wave scattering length (positive for repulsive interaction and negative for attractive interaction). It is necessary to ensure that the wave function is properly normalized. Specifically, we require

$$\int_{\mathbb{R}^3} |\psi(\mathbf{x},t)|^2\, d\mathbf{x} = 1. \quad (77)$$

5.1 Dimensionless GPE

In order to scale the Eq. (76) under the normalization (77), we introduce

$$\tilde{t} = \omega_x t, \quad \tilde{\mathbf{x}} = \frac{\mathbf{x}}{a_0}, \quad \tilde{\psi}(\tilde{\mathbf{x}},\tilde{t}) = a_0^{3/2}\psi(\mathbf{x},t), \quad \text{with} \quad a_0 = \sqrt{\hbar/\omega_x m}, \quad (78)$$

where a_0 is the length of the harmonic oscillator ground state. In fact, here we choose $1/\omega_x$ and a_0 as the dimensionless time and length units, respectively.

Plugging (78) into (76), multiplying by $1/m\omega_x^2 a_0^{1/2}$, and then removing all $\tilde{}$, we get the following dimensionless GPE under the normalization (77) in three dimension

$$i\,\frac{\partial\psi(\mathbf{x},t)}{\partial t} = -\frac{1}{2}\nabla^2\psi(\mathbf{x},t) + V(\mathbf{x})\psi(\mathbf{x},t) + \beta\,|\psi(\mathbf{x},t)|^2\psi(\mathbf{x},t), \tag{79}$$

where

$$V(\mathbf{x}) = \frac{1}{2}\left(x^2 + \gamma_y^2 y^2 + \gamma_z^2 z^2\right),\ \gamma_y = \frac{\omega_y}{\omega_x},\ \gamma_z = \frac{\omega_z}{\omega_x},\ \beta = \frac{U_0 N}{a_0^3\hbar\omega_x} = \frac{4\pi a_s N}{a_0}.$$

There are two extreme regimes of the interaction parameter β: (1) $\beta = o(1)$, the Eq. (79) describes a weakly interacting condensation; (2) $\beta \gg 1$, it corresponds to a strongly interacting condensation or to the semiclassical regime. There are two extreme regimes between the trap frequencies: (1) $\gamma_y \approx 1$ and $\gamma_z \gg 1$, it is a disk-shaped condensation; (2) $\gamma_y \gg 1$ and $\gamma_z \gg 1$, it is a cigar-shaped condensation.

5.2 Reduction to lower dimension

In the following two cases, the 3d GPE (79) can approximately be reduced to 2d or even 1d [35, 5, 2]. In the case (disk-shaped condensation)

$$\omega_x \approx \omega_y, \quad \omega_z \gg \omega_x, \qquad \Longleftrightarrow \quad \gamma_y \approx 1, \quad \gamma_z \gg 1,$$

the 3d GPE (79) can be reduced to 2d GPE with $\mathbf{x} = (x, y)$ by assuming that the time evolution does not cause excitations along the z-axis since they have a large energy of approximately $\hbar\omega_z$ compared to excitations along the x and y-axis with energies of about $\hbar\omega_x$. Thus we may assume that the condensation wave function along the z-axis is always well described by the harmonic oscillator ground state wave function and set

$$\psi = \psi_2(x, y, t)\psi_{\rm ho}(z) \qquad \text{with} \quad \psi_{\rm ho}(z) = (\gamma_z/\pi)^{1/4}\, e^{-\gamma_z z^2/2}. \tag{80}$$

Plugging (80) into (79), then multiplying by $\psi_{\rm ho}^*(z)$ (where f^* denotes the conjugate of a function f), integrating with respect to z over $(-\infty, \infty)$, we get

$$i\,\frac{\partial\psi_2(\mathbf{x},t)}{\partial t} = -\frac{1}{2}\nabla^2\psi_2 + \frac{1}{2}\left(x^2 + \gamma_y^2 y^2 + C\right)\psi_2 + \beta_2|\psi_2|^2\psi_2, \tag{81}$$

where

$$\beta_2 = \beta\int_{-\infty}^{\infty}\psi_{\rm ho}^4(z)\,dz = \beta\sqrt{\frac{\gamma_z}{2\pi}},\ C = \int_{-\infty}^{\infty}\left(\gamma_z^2 z^2|\psi_{\rm ho}(z)|^2 + \left|\frac{d\psi_{\rm ho}}{dz}\right|^2\right)\,dz.$$

Since this GPE is time-transverse invariant, we can replace $\psi_2 \to \psi\ e^{-i\frac{Ct}{2}}$ which drops the constant C in the trap potential and obtain the 2d GPE, i.e.

$$i\,\frac{\partial\psi(\mathbf{x},t)}{\partial t} = -\frac{1}{2}\nabla^2\psi + \frac{1}{2}\left(x^2+\gamma_y^2y^2\right)\psi + \beta_2|\psi|^2\psi. \tag{82}$$

The observables are not affected by this.

In the case (cigar-shaped condensation) [35, 5, 2]

$$\omega_y \gg \omega_x, \quad \omega_z \gg \omega_x, \qquad \Longleftrightarrow \quad \gamma_y \gg 1, \quad \gamma_z \gg 1,$$

the 3d GPE (79) can be reduced to 1d GPE with $\mathbf{x} = x$. Similarly to the 2d case, we derive the 1d GPE [35, 5, 2]

$$i\,\frac{\partial\psi(x,t)}{\partial t} = -\frac{1}{2}\psi_{xx}(x,t) + \frac{x^2}{2}\psi(x,t) + \beta_1|\psi(x,t)|^2\psi(x,t), \tag{83}$$

where $\beta_1 = \beta\sqrt{\gamma_y\gamma_z}/2\pi$.

In fact, the 3d GPE (79), 2d GPE (82) and 1d GPE (83) can be written in a unified way

$$i\,\frac{\partial\psi(\mathbf{x},t)}{\partial t} = -\frac{1}{2}\nabla^2\psi + V_d(\mathbf{x})\psi + \beta_d\,|\psi|^2\psi, \quad \mathbf{x}\in\mathbb{R}^d, \tag{84}$$

where

$$\beta_d = \beta\begin{cases}\sqrt{\gamma_y\gamma_z}/2\pi, \\ \sqrt{\gamma_z/2\pi}, \\ 1,\end{cases} \qquad V_d(\mathbf{x}) = \begin{cases} x^2/2, & d=1, \\ \left(x^2+\gamma_y^2y^2\right)/2, & d=2, \\ \left(x^2+\gamma_y^2y^2+\gamma_z^2z^2\right)/2, & d=3.\end{cases} \tag{85}$$

The normalization condition to (84) is

$$\int_{\mathbb{R}^d} |\psi(\mathbf{x},t)|^2\,d\mathbf{x} = 1. \tag{86}$$

Two important invariants of (84) are the **normalization of the wave function**

$$N(\psi) = \int_{\mathbb{R}^d} |\psi(\mathbf{x},t)|^2\,d\mathbf{x} = 1, \qquad t\ge 0 \tag{87}$$

and the **energy**

$$E_\beta(\psi) = \int_{\mathbb{R}^d}\left[\frac{1}{2}|\nabla\psi(\mathbf{x},t)|^2 + V_d(\mathbf{x})|\psi(\mathbf{x},t)|^2 + \frac{\beta_d}{2}|\psi(\mathbf{x},t)|^4\right]d\mathbf{x},\ t\ge 0. \tag{88}$$

5.3 Ground state solution

To find a stationary solution of (84), we write

$$\psi(\mathbf{x},t) = e^{-i\mu t}\,\phi(\mathbf{x}), \tag{89}$$

where μ is the chemical potential of the condensation and ϕ a function independent of time. Inserting into (84) gives the following equation for $\phi(\mathbf{x})$

$$\mu\ \phi(\mathbf{x}) = -\frac{1}{2}\nabla^2\phi(\mathbf{x}) + V_d(\mathbf{x})\phi(\mathbf{x}) + \beta_d\ |\phi(\mathbf{x})|^2\phi(\mathbf{x}), \qquad \mathbf{x} \in \mathbb{R}^d, \tag{90}$$

under the normalization condition

$$\int_{\mathbb{R}^d} |\phi(\mathbf{x})|^2\ d\mathbf{x} = 1. \tag{91}$$

This is a nonlinear eigenvalue problem under a constraint and any eigenvalue μ can be computed from its corresponding eigenfunction ϕ by

$$\begin{aligned}\mu = \mu_\beta(\phi) &= \int_{\mathbb{R}^d} \left[\frac{1}{2}|\nabla\phi(\mathbf{x})|^2 + V_d(\mathbf{x})|\phi(\mathbf{x})|^2 + \beta_d\ |\phi(\mathbf{x})|^4\right]\ d\mathbf{x} \\ &= E_\beta(\phi) + \frac{\beta_d}{2}\int_{\mathbb{R}^d} |\phi(\mathbf{x})|^4\ d\mathbf{x}.\end{aligned} \tag{92}$$

The Bose-Einstein condensation ground state solution $\phi_g(\mathbf{x})$ is found by minimizing the energy functional $E_\beta(\phi)$ under the constraint (91), i.e. to compute the ground state ϕ_g, we solve the minimization problem
(V) Find $(\mu_g, \phi_g \in V)$ such that

$$E_\beta(\phi_g) = \min_{\phi\in V}\ E_\beta(\phi), \qquad \mu_g = \mu_\beta(\phi_g) = E_\beta(\phi_g) + \frac{\beta_d}{2}\int_{\mathbb{R}^d} |\phi_g(\mathbf{x})|^4\ d\mathbf{x}, \tag{93}$$

where the set V is defined as

$$V = \{\phi \mid E_\beta(\phi) < \infty, \quad \|\phi(\mathbf{x})\| = 1\}, \quad \|\phi\|^2 = \|\phi\|^2_{L^2} = \int_{\mathbb{R}^d} |\phi(\mathbf{x})|^2\ d\mathbf{x}.$$

In non-rotating BEC, the minimization problem (93) has a unique real valued nonnegative ground state solution $\phi_g(\mathbf{x}) > 0$ for $\mathbf{x} \in \mathbb{R}^d$ [37].

Various algorithms for computing the minimizer of the minimization problem (93) have been studied in the literature. For instance, second order in time discretization scheme that preserves the normalization and energy diminishing properties were presented in [1]. Perhaps one of the more popular technique for dealing with the normalization constraint (91) is through the following construction: choose a time sequence $0 = t_0 < t_1 < t_2 < \cdots < t_n < \cdots$ with $\Delta t_n = t_{n+1} - t_n > 0$ and $k = \max_{n\geq 0}\ \Delta t_n$. To adapt an algorithm for the solution of the usual gradient flow to the minimization problem under a constraint, it is natural to consider the following splitting (or projection) scheme which was widely used in physical literatures [12, 1] for computing the ground state solution of BEC:

$$\phi_t = -\frac{1}{2}\frac{\delta E_\beta(\phi)}{\delta\phi} = \frac{1}{2}\nabla^2\phi - V_d(\mathbf{x})\phi - \beta_d\ |\phi|^2\phi,$$

$$\mathbf{x} \in \mathbb{R}^d,\ t_n < t < t_{n+1},\ n \geq 0, \tag{94}$$

$$\phi(x, t_{n+1}) \stackrel{\triangle}{=} \phi(\mathbf{x}, t^+_{n+1}) = \frac{\phi(\mathbf{x}, t^-_{n+1})}{\|\phi(\cdot, t^-_{n+1})\|}, \qquad \mathbf{x} \in \mathbb{R}^d, \quad n \geq 0, \tag{95}$$

$$\phi(\mathbf{x}, 0) = \phi_0(\mathbf{x}), \quad \mathbf{x} \in \mathbb{R}^d \qquad \text{with} \qquad \|\phi_0\| = 1; \tag{96}$$

where $\phi(\mathbf{x}, t_n^{\pm}) = \lim_{t \to t_n^{\pm}} \phi(\mathbf{x}, t)$. In fact, the gradient flow (94) can be viewed as applying the steepest decent method to the energy functional $E_\beta(\phi)$ without constraint and (95) then projects the solution back to the unit sphere in order to satisfying the constraint (91). From the numerical point of view, the gradient flow (94) can be solved via traditional techniques and the normalization of the gradient flow is simply achieved by a projection at the end of each time step. For $\beta_d = 0$, as observed in [4], the gradient flow with discrete normalization (GFDN) (94)-(96) preserves the energy diminishing property:

Theorem 2. *Suppose $V_d(\mathbf{x}) \geq 0$ for all $\mathbf{x} \in \mathbb{R}^d$. For $\beta_d = 0$, the GFDN (94)-(96) is energy diminishing for any time step $k > 0$ and initial data ϕ_0, i.e.*

$$E_0(\phi(\cdot, t_{n+1})) \leq E_0(\phi(\cdot, t_n)) \leq \cdots \leq E_0(\phi(\cdot, 0)) = E_0(\phi_0), \quad n \geq 0. \tag{97}$$

In fact, the normalized step (95) is equivalent to solve the following ODE *exactly*

$$\phi_t(\mathbf{x}, t) = \mu_\phi(t, k)\phi(\mathbf{x}, t), \qquad \mathbf{x} \in \mathbb{R}^d, \quad t_n < t < t_{n+1}, \quad n \geq 0, \tag{98}$$

$$\phi(\mathbf{x}, t_n^+) = \phi(\mathbf{x}, t_{n+1}^-), \qquad \mathbf{x} \in \mathbb{R}^d; \tag{99}$$

where

$$\mu_\phi(t, k) \equiv \mu_\phi(t_{n+1}, \Delta t_n) = -\frac{1}{2\,\Delta t_n} \ln \|\phi(\cdot, t_{n+1}^-)\|^2, \qquad t_n \leq t \leq t_{n+1}.$$

Thus the GFDN (94)-(96) can be viewed as a first-order splitting method for the gradient flow with discontinuous coefficients:

$$\phi_t = \frac{1}{2}\nabla^2\phi - V(\mathbf{x})\phi - \beta\,|\phi|^2\phi + \mu_\phi(t, k)\phi, \qquad \mathbf{x} \in \mathbb{R}^d, \quad t \geq 0, \tag{100}$$

$$\phi(\mathbf{x}, 0) = \phi_0(\mathbf{x}), \qquad \mathbf{x} \in \mathbb{R}^d \qquad \text{with} \qquad \|\phi_0\| = 1. \tag{101}$$

Let $k \to 0$, we see that

$$\begin{aligned} \mu_\phi(t) &= \lim_{k \to 0^+} \mu_\phi(t, k) \\ &= \frac{1}{\|\phi(\cdot, t)\|^2} \int_{\mathbb{R}^d} \left[\frac{1}{2} |\nabla \phi(\mathbf{x}, t)|^2 + V_d(\mathbf{x})\phi^2(\mathbf{x}, t) + \beta_d \phi^4(\mathbf{x}, t) \right] d\mathbf{x}. \end{aligned}$$

This suggests us to consider the following continuous normalized gradient flow (CNGF):

$$\phi_t = \frac{1}{2}\nabla^2\phi - V_d(\mathbf{x})\phi - \beta_d\,|\phi|^2\phi + \mu_\phi(t)\phi, \qquad \mathbf{x} \in \mathbb{R}^d, \quad t \geq 0, \tag{102}$$

$$\phi(\mathbf{x}, 0) = \phi_0(\mathbf{x}), \qquad \mathbf{x} \in \mathbb{R}^d \qquad \text{with} \qquad \|\phi_0\| = 1. \tag{103}$$

In fact, the right hand side of (102) is the same as (90) if we view $\mu_\phi(t)$ as a Lagrange multiplier for the constraint (91). Furthermore for the above CNGF, as observed in [4], the solution of (102) also satisfies the following theorem which provides a mathematical justification for the algorithm (94)-(96):

Theorem 3. *Suppose $V_d(\mathbf{x}) \geq 0$ for all $\mathbf{x} \in \mathbb{R}^d$ and $\beta_d \geq 0$. Then the CNGF (102)-(103) is normalization conservation and energy diminishing, i.e.*

$$\|\phi(\cdot,t)\|^2 = \int_{\mathbb{R}^d} |\phi(\mathbf{x},t)|^2 \, d\mathbf{x} = \|\phi_0\|^2 = 1, \qquad t \geq 0, \tag{104}$$

$$\frac{d}{dt} E_\beta(\phi) = -2 \left\|\phi_t(\cdot,t)\right\|^2 \leq 0 \,, \qquad t \geq 0, \tag{105}$$

which in turn implies

$$E_\beta(\phi(\cdot,t_1)) \geq E_\beta(\phi(\cdot,t_2)), \qquad 0 \leq t_1 \leq t_2 < \infty.$$

In fact, it is easy to prove that eigenfunctions of the nonlinear eigenvalue problem (90) under the constraint (91), critical points of the energy functional $E_\beta(\phi)$ under the constraint (91) and steady state solutions of the CNGF (102)-(103) are equivalent.

Here we present a backward Euler finite difference (BEFD) scheme for fully discretizing the GFDN (94)-(96) to compute the ground state solutions of BEC. For simplicity of notation we introduce the methods for the case of one spatial dimension ($d = 1$). Generalizations to higher dimension are straightforward for tensor product grids and the results remain valid without modifications. In 1d, we choose an interval $[a, b]$ with $|a|$, b sufficiently large and spatial mesh size $h = \Delta x > 0$ with $h = (b-a)/M$ and M an even positive integer, and define grid points and time steps by

$$x_j := a + j\, h, \qquad t_n := n\, k, \qquad j = 0, 1, \cdots, M, \qquad n = 0, 1, 2, \cdots$$

Let ϕ_j^n be the numerical approximation of $\phi(x_j, t_n)$. We use backward Euler for time discretization and second-order centered finite difference for spatial derivatives. The detail scheme is:

$$\begin{aligned}
&\frac{\phi_j^* - \phi_j^n}{k} = \frac{\phi_{j+1}^* - 2\phi_j^* + \phi_{j-1}^*}{2h^2} - V_1(x_j)\phi_j^* - \beta_1 \left(\phi_j^n\right)^2 \phi_j^*, \ 1 \leq j \leq M-1, \\
&\phi_0^* = \phi_M^* = 0, \qquad \phi_j^0 = \phi_0(x_j), \qquad j = 0, 1, \cdots, M, \\
&\phi_j^{n+1} = \frac{\phi_j^*}{\|\phi^*\|}, \qquad j = 0, \cdots, M, \qquad n = 0, 1, \cdots;
\end{aligned} \tag{106}$$

where the norm is defined as $\|\phi^*\|^2 = h \sum_{j=1}^{M-1} \left(\phi_j^*\right)^2$. When $V_1(x) \geq 0$, as observed in [4], this scheme is monotone for $\beta_1 \geq 0$ and energy diminishing for $\beta_1 = 0$ for any time step $k > 0$. For non-rotating BEC with harmonic oscillator potential, the above scheme can be used to compute the ground (first excited) state provided that we chose the initial data $\phi_0(x)$ as an even positive (odd) function, e.g. $\phi_0(x) = \frac{1}{\pi^{1/4}} e^{-x^2/2}$ ($\phi_0(x) = \frac{x\sqrt{2}}{\pi^{1/4}} e^{-x^2/2}$). Figure 13 shows the ground state $\phi_g(x)$ and first excited state $\phi_1(x)$ of BEC in 1d with $V_1(x) = x^2/2$ in (84) for different β_1. For more numerical results of ground states in 1d, 2d and 3d BEC, we refer [4, 9, 2].

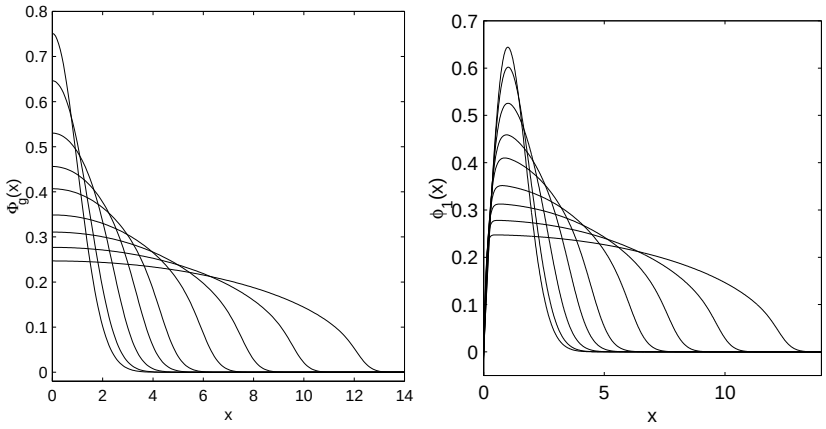

Fig. 13. Stationary states of BEC in 1d for $\beta_1 = 0, 3.1371, 12.5484, 31.371, 62.742, 156.855, 313.71, 627.42, 1254.8$ (with decreasing peak). Left: ground state $\phi_g(x)$ (positive even function); Right: first excited state $\phi_1(x)$ (odd function).

5.4 Time-splitting spectral method for GPE

To study the dynamics of BEC, one needs to solve the time-dependent GPE (84) numerically. Here we present the time-splitting spectral method introduced in [5, 3, 2] for the GPE (84). Similarly, we only introduce the method in one space dimension ($d = 1$). Generalizations to $d > 1$ are straightforward for tensor product grids and the results remain valid without modifications. For $d = 1$, the equation (84) with homogeneous Dirichlet boundary conditions becomes

$$i\frac{\partial\psi(x,t)}{\partial t} = -\frac{1}{2}\psi_{xx} + V_1(x)\psi + \beta_1|\psi|^2\psi, \qquad a < x < b, \tag{107}$$

$$\psi(x, t = 0) = \psi_0(x), \ a \le x \le b, \qquad \psi(a,t) = \psi(b,t) = 0, , \ t > 0. \tag{108}$$

Let ψ_j^n be the approximation of $\psi(x_j, t_n)$.From time $t = t_n$ to $t = t_{n+1}$, the GPE (107) is solved in two splitting steps. One solves first

$$i\psi_t = -\frac{1}{2}\psi_{xx}, \tag{109}$$

for the time step of length k, followed by solving

$$i\frac{\partial\psi(x,t)}{\partial t} = V_1(x)\psi(x,t) + \beta_1|\psi(x,t)|^2\psi(x,t), \tag{110}$$

for the same time step. Equation (109) will be discretized in space by the sine spectral method and integrated in time *exactly*. For $t \in [t_n, t_{n+1}]$, the ODE (110) leaves $|\psi|$ invariant in t [7, 8] and therefore becomes

$$i\frac{\partial\psi(x,t)}{\partial t} = V_1(x)\psi(x,t) + \beta_1|\psi(x,t_n)|^2\psi(x,t) \tag{111}$$

and thus can be integrated *exactly*. We combine the splitting steps via the fourth-order split-step method and obtain a fourth-order time-splitting sine-spectral method (**TSSP4**) for GPE (107). The detailed method is given by

$$\begin{aligned}
\psi_j^{(1)} &= e^{-i2w_1k(V_1(x_j)+\beta_1|\psi_j^n|^2))}\ \psi_j^n,\\
\psi_j^{(2)} &= \sum_{l=1}^{M-1} e^{-iw_2k\mu_l^2}\ \widehat{\psi}_l^{(1)}\ \sin(\mu_l(x_j-a)),\\
\psi_j^{(3)} &= e^{-i2w_3k(V_1(x_j)+\beta_1|\psi_j^{(2)}|^2))}\ \psi_j^{(2)},\\
\psi_j^{(4)} &= \sum_{l=1}^{M-1} e^{-iw_4k\mu_l^2}\ \widehat{\psi}_l^{(3)}\ \sin(\mu_l(x_j-a)), \qquad j=1,2,\cdots,M-1,\\
\psi_j^{(5)} &= e^{-i2w_3k(V_1(x_j)+\beta_1|\psi_j^{(4)}|^2))}\ \psi_j^{(4)},\\
\psi_j^{(6)} &= \sum_{l=1}^{M-1} e^{-iw_2k\mu_l^2}\ \widehat{\psi}_l^{(5)}\ \sin(\mu_l(x_j-a)),\\
\psi_j^{n+1} &= e^{-i2w_1k(V_1(x_j)+\beta_1|\psi_j^{(6)}|^2))}\ \psi_j^{(6)};
\end{aligned} \tag{112}$$

where $w_1 = 0.33780\ 17979\ 89914\ 40851$, $w_2 = 0.67560\ 35959\ 79828\ 81702$, $w_3 = -0.08780\ 17979\ 89914\ 40851$ and $w_4 = -0.85120\ 71979\ 59657\ 63405$ [49], and $\widehat{U}_l$, the sine-transform coefficients of a complex vector $U = (U_0, U_1, \cdots, U_M)$ with $U_0 = U_M = \mathbf{0}$, are defined as

$$\mu_l = \frac{\pi l}{b-a}, \quad \widehat{U}_l = \frac{2}{M}\sum_{j=1}^{M-1} U_j\ \sin(\mu_l(x_j-a)),\ l=1,2,\cdots,M-1, \tag{113}$$

with

$$\psi_j^0 = \psi(x_j,0) = \psi_0(x_j), \qquad j=0,1,2,\cdots,M. \tag{114}$$

Note that the only time discretization error of TSSP4 is the splitting error, which is fourth order in k. As observed in [5, 3, 2], the scheme is explicit, unconditionally stable, of spectral order accuracy in space and fourth order accuracy in time, and conserves the position density. Furthermore, it is time reversible and time transverse invariant, just as they hold for the GPE itself. Figure 14 plots the condensate width $\sigma_x(t) = \|x\psi\|$, central density $\psi(0,t)|^2$ as functions of time and evolution of the density $|\psi|^2$ in space-time for 1d GPE (84) with $V_1(x) = 2^2x^2/2$, $\beta_1 = 20$ and $\psi_0(x)$ be the ground state solution of (84) with $d = 1$, $V_1(x) = x^2/2$ and $\beta_1 = 20$. The above time-splitting spectral method can be easily extended to GPE with a quintic damping term for modeling a collapse and explosion BEC [3, 6] observed in experiment [18]. In the experiment, the s-wave scattering length is changed by an external magnetic

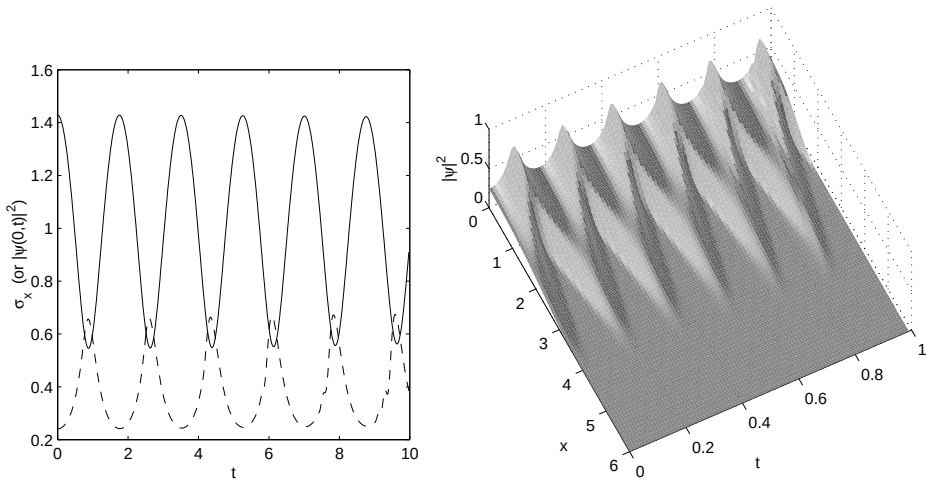

Fig. 14. Dynamics of 1d BEC. Left: Width of the condensate σ_x ('—') and central density $|\psi(0,t)|^2$ ('- - -'); Right: Evolution of the density function $|\psi|^2$.

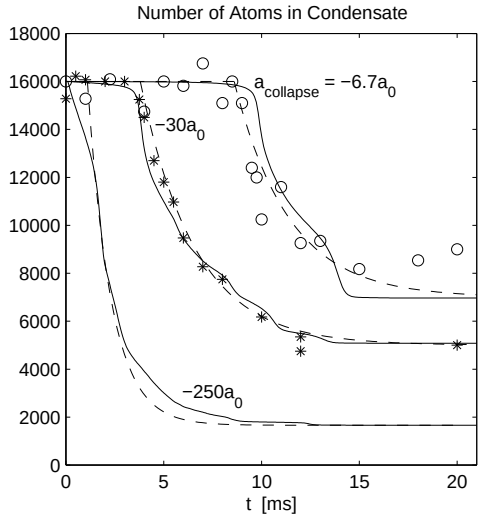

Fig. 15. Number of remaining atoms after collapsing a ^{85}Rb condensate of $N_0 = 16000$ atoms. Collapse is achieved by ramping the scattering length linearly from $a_{\rm init} = 7a_0$ (where a_0 is the Bohr radius) to $a_{\rm collapse} = -6.7a_0, -30a_0$ and $-250a_0$ in 0.1 [ms] as a function of time $\tau_{\rm evolve}$ [ms] (labelled as t). The '*' and 'o' are taken from the experiment [18], the solid curves are our numerical solutions and the dashed curves are fitted to the experimental points: $N_{\rm total}(t) = N_{\rm remnant}(\tau_{\rm evolve}) = N^0_{\rm remnant} + (N_0 - N^0_{\rm remnant}) \cdot \exp((t_{\rm collapse} - \tau_{\rm evolve})/t_{\rm decay})$ with $N^0_{\rm remnant} = 7000,\ 5000,\ 1660$; $t_{\rm collapse} = 8.6,\ 3.8,\ 1.1$ [ms] and $t_{\rm decay} = 2.8,\ 2.8,\ 1.2$ [ms] for $a_{\rm collapse} = -6.7a_0,\ -30a_0,\ -250a_0$, respectively.

field near a Feshbach resonance of the ^{85}Rb atoms, i.e. $a_s = a_s(t)$. They started from a stable condensate with a positive scattering length $a_s = a_{\text{init}} > 0$, then changed a_s from positive to negative $a_s = a_{\text{collapse}} < 0$, and observed a series collapse and explosion. Figure 15 plots the number of remaining atoms after collapsing a ^{85}Rb condensate of initially $N_0 = 16000$ atoms with different a_{collapse} [6]. For more numerical results of dynamics in 1d, 2d and 3d BEC, we refer [2, 5, 6].

6 Coupling Quantum Boltzmann and Gross-Pitaevskii equations

As already mentioned in the introduction the process of creating a Bose-Einstein condensate in a trap by means of evaporative cooling starts in a regime covered by the QBE and finishes in a regime where the Gross-Pitaevskii (GPE) equation is expected to be valid. The GPE is capable to describe the main properties of the condensate at very low temperatures, it treats the condensate as a classical field and neglects quantum and thermal fluctuations. As a consequence the theory breaks down at higher temperatures where the non condensed fraction of the gas cloud is significant. An approach which allows the treatment of both condensate and noncondensate parts simultaneously was developed in [50].

The resulting equations of motion reduce to a generalized GPE for the condensate wave function coupled with a semiclassical QBE for the thermal cloud:

$$i\hbar\frac{\partial}{\partial t}\psi(\mathbf{x},t) = -\frac{\hbar^2}{2m}\nabla^2\psi(\mathbf{x},t) + V(\mathbf{x})\psi(\mathbf{x},t) + [U_0(n_c(\mathbf{x},t) + 2n(\mathbf{x},t)) - iR(\mathbf{x},t)]\psi(\mathbf{x},t), \tag{115}$$

$$\frac{\partial F}{\partial t} + \frac{\mathbf{p}}{m}\cdot\nabla_{\mathbf{x}}F - \nabla_{\mathbf{x}}U\cdot\nabla_{\mathbf{p}}F = Q(F) + Q_c(F). \tag{116}$$

where $n_c(\mathbf{x},t) = |\psi(\mathbf{x},t)|^2$ is the condensate density, $V(\mathbf{x})$ is the confining potential. The collision integral $Q(F)$ is the conventional QBE integral whereas $Q_c(F)$ describes collisions between condensate and non condensate particles and is given by

$$\frac{\sigma n_c}{m^2\pi}\int_{\mathbb{R}^9}\delta(m\mathbf{v}_c + \mathbf{p}_* - \mathbf{p}' - \mathbf{p}'_*)\delta(\varepsilon_c + \varepsilon_* - \varepsilon' - \varepsilon'_*)[\delta(\mathbf{p}-\mathbf{p}_*) - \delta(\mathbf{p}-\mathbf{p}') - \delta(\mathbf{p}-\mathbf{p}'_*)][F'F'_*(1+F_*) - F_*(1+F')(1+F'_*)]\,d\mathbf{p}_*d\mathbf{p}'d\mathbf{p}'_*, \tag{117}$$

with $\sigma = 8\pi a_s^2$, $\varepsilon = \mathbf{p}^2/2 + U(\mathbf{x},t)$ where $U = V + 2U_0(n_c + n)$ is the mean field potential. The presence of $Q_c(F)$ leads to a change in the number of condensate particles. $n(\mathbf{x},t)$ and $R(\mathbf{x},t)$ are the non condensate density and a source term, respectively, which are defined as

$$n(\mathbf{x},t) = \frac{1}{(2\pi\hbar)^3}\int F(\mathbf{x},\mathbf{p},t)\,d\mathbf{p},\;\; R(\mathbf{x},t) = \frac{\hbar}{2n_c(2\pi\hbar)^3}\int Q_c(F)d\mathbf{p}. \quad (118)$$

Note that for low temperatures $T \to 0$ we have $n, R \to 0$ and we recover the conventional GPE. The equations (115), (116) are normalized as $N_c(0) = N_c^0$ and $N_t(0) = N_t^0$ with

$$N_c(t) = \int_{\mathbb{R}^3} |\psi(\mathbf{x},t)|^2\,d\mathbf{x}, \qquad N_t(t) = \int_{\mathbb{R}^3} |n(\mathbf{x},t)|^2\,d\mathbf{x}, \qquad t \geq 0, \quad (119)$$

where N_c^0 and N_t^0 are the number of particles in the condensate and thermal cloud at time $t = 0$, respectively. It is easy to see from the equations (115), (116) that

$$\frac{dN_t(t)}{dt} = \frac{1}{(2\pi\hbar)^3}\int_{\mathbb{R}^6} Q_c(F)d\mathbf{p}\,d\mathbf{x} = -\frac{dN_c(t)}{dt}, \qquad t \geq 0. \quad (120)$$

As a consequence the total number of particles defined as $N_{\rm total}(t) = N_c(t) + N_t(t) \equiv N_{\rm total}^0 = N_c^0 + N_t^0$ is obviously conserved. This set of equations has been solved numerically in [32] by combining a Monte Carlo method for the kinetic equations with a Fourier spectral method for the GPE. We hope to present results for such system based on coupling the methods derived in the previous sections for the kinetic part and the GPE solver [5, 40].

Acknowledgement

The authors are grateful to Dieter Jaksch for stimulating discussions on the subject of this work. This work was supported by the WITTGENSTEIN AWARD 2000 of Peter Markowich, financed by the Austrian Research Fund FWF and by the European network HYKE, funded by the EC as contract HPRN-CT-2002-00282.

References

1. A. Aftalion, and Q. Du, Vortices in a rotating Bose-Einstein condensate: Critical angular velocities and energy diagrams in the Thomas-Fermi regime, Phys. Rev. A, **64**, 063603, (2001).
2. W. Bao, Ground states and dynamics of multi-component Bose-Einstein condensates, arXiv: cond-mat/0305309.
3. W. Bao, D. Jaksch, An explicit unconditionally stable numerical methods for solving damped nonlinear Schrodinger equations with a focusing nonlinearity, *SIAM J. Numer. Anal.*, to appear (arXiv: math.NA/0303158).
4. W. Bao and Q. Du, Computing the ground state solution of Bose-Einstein condensates by a normalized gradient flow, *SIAM J. Sci. Comp.*, to appear (arXiv: cond-mat/0303241).

5. W.Bao, D.Jaksch, P.Markowich, Numerical solution of the Gross-Pitaevskii Equation for Bose-Einstein condensation, *J. Comput. Phys.*, **187**, 318 - 342, (2003).
6. W.Bao, D.Jaksch, P.Markowich, Three Dimensional Simulation of Jet Formation in Collapsing Condensates, arXiv: cond-mat/0307344.
7. W. Bao, S. Jin and P.A. Markowich, On time-splitting spectral approximations for the Schrödinger equation in the semiclassical regime, *J. Comput. Phys.*, **175**, 487-524, (2002).
8. W. Bao, S. Jin and P.A. Markowich, Numerical study of time-splitting spectral discretizations of nonlinear Schrödinger equations in the semi-clasical regimes, *SIAM J. Sci. Comp.*, to appear.
9. W. Bao and W. Tang, Ground state solution of trapped interacting Bose-Einstein condensate by directly minimizing the energy functional, *J. Comput. Phys.*, **187**, 230-254, (2003).
10. D.Benedetto, F. Castella, R. Esposito, M. Pulvirenti, Some Considerations on the derivation of the nonlinear Quantum Boltzmann Equation. *Mathematical Physics Archive*, University of Texas, 03-19, (2003).
11. S.N. Bose, Plancks Gesetz and Lichtquantenhypothese, *Z. Phys.*, **26**, 178–181, (1924).
12. M.L. Chiofalo, S. Succi and M.P. Tosi, Ground state of trapped interacting Bose-Einstein condensates by an explicit imaginary-time algorithm, *Phys. Rev. E*, **62**, 7438-7444, (2000).
13. C. Buet, S. Cordier, Numerical method for the Compton scattering operator, *Lecture Notes on the discretization of the Boltzmann equation*, ed. N.Bellomo, World Scientific, (2002).
14. C. Buet, S. Cordier, P. Degond and M. Lemou, Fast algorithms for numerical, conservative, and entropy approximations of the Fokker-Planck equation, *J. Comp. Phys.*, **133**, 310-322, (1997).
15. S. Chapman and T. G. Cowling, *The mathematical theory of non- uniform gases*, Cambridge University Press, 1970. Third edition.
16. E. A. Cornell, J. R. Ensher and C. E. Wieman, Experiments in dilute atomic Bose-Einstein condensation in *Bose-Einstein Condensation in Atomic Gases*, Proceedings of the International School of Physics Enrico Fermi Course CXL (M. Inguscio, S. Stringari and C. E. Wieman, Eds., Italian Physical Society, 1999), pp. 15-66 (cond-mat/9903109).
17. P.J.Davis, P.Rabinowitz, *Methods of numerical integration*, Academic Press, (1975).
18. E.A. Donley, N.R. Claussen, S.L. Cornish, J.L. Roberts, E.A. Cornell and C.E. Wieman, Dynamics of collapsing and exploding Bose-Einstein condensates, Nature, 412, 295-299, 2001.
19. A.Einstein, Quantentheorie des einatomingen idealen gases, *Stiz. Presussische Akademie der Wissenshaften Phys-math. Klasse*, Sitzungsberichte, **23**, 1–14, (1925).
20. A.Einstein, Zur quantentheorie des idealen gases, *Stiz. Presussische Akademie der Wissenshaften Phys-math. Klasse*, Sitzungsberichte, **23**, 18–25, (1925).
21. L. Erdös, M. Salmhofer, H.Yau, On the quantum Boltzmann equation, preprint 2003
22. M. Escobedo, S. Mischler, Equation de Boltzmann quantique homogene: existence et comportement asymptotique, *C. R. Acad. Sci.* Paris 329 Serie I, 593–598 (1999)

23. M.Escobedo, S.Mischler, M.A.Valle, Homogeneous Boltzmann equation in quantum relativistic kinetic theory, *Electronic Journal of Differential Equations*, Monograph 04, 2003, 85 pages. (http://ejde.math.swt.edu or http://ejde.math.unt.edu).
24. M.Escobedo, S.Mischler, On a quantum Boltzmann equation for a gas of photons, *J. Math. Pures Appl.*, **9** 80, 471–515, (2001).
25. C.W.Gardiner, D.Jaksch, P.Zoller, Quantum Kinetic Theory II: Simulation of the Quantum Boltzmann Master Equation, *Phys. Rev. A*, **56**, 575, (1997)
26. C.W.Gardiner, P.Zoller, Quantum Kinetic Theory I: A Quantum Kinetic Master Equation for Condensation of a weakly interacting Bose gas without a trapping potential, *Phys. Rev. A*, **55**, 2902, (1997),
27. C.W.Gardiner, P.Zoller, Quantum Kinetic Theory III: Quantum kinetic master equation for strongly condensed trapped systems, *Phys. Rev. A*, **58**, 536, (1998)
28. V.L. Ginzburg, L.P. Pitaevskii, Zh. Eksp. Teor.Fiz. 34, 1240 (1958) [Sov. Phys. JETP 7, 858 (1958)]
29. E.P. Gross, J. Math. Phys. 4, 195 (1963).
30. E.P. Gross, *Nuovo. Cimento.*, **20**, 454, (1961).
31. D.Jaksch, P.Markowich, L.Pareschi, M.Wenin, P.Zoller, Increasing phase-space density by varying the trap potential, work in progress.
32. B.Jackson, E.Zaremba, *Dynamical simulations of trapped Bose gases at finite temperatures*, preprint 2002 (cond-mat/0106652).
33. W. Ketterle, D.S. Durfee, D.M. Stamper-Kurn, Making, probing and understanding Bose-Einstein condensates, in *Bose-Einstein condensation in atomic gases*, Proceedings of the International School of Physics Enrico Fermi, Course CXL, edited by M. Inguscio, S. Stringari, and C.E. Wieman (IOS Press, Amsterdam, 1999), pp. 67176 (cond-mat/9904034).
34. L. Landau and E. Lifschitz, Quantum Mechanics: non-relativistic theory, Pergamon Press, New York, (1977).
35. P. Leboeuf and N. Pavloff, Phys. Rev. A **64**, 033602 (2001); V. Dunjko, V. Lorent, and M. Olshanii, Phys. Rev. Lett. **86**, 5413 (2001).
36. M.Lemou, Multipole expansions for the Fokker-Planck-Landau operator, *Numerische Mathematik*, **78**, 597–618, (1998).
37. E.H. Lieb, R. Seiringer and J. Yngvason, Bosons in a Trap: A Rigorous Derivation of the Gross-Pitaevskii Energy Functional, *Phys. Rev. A*, **61**, 3602, (2000).
38. X.Lu, On spatially homogeneous solutions of a modified Boltzmann equation for Fermi-Dirac particles, *J. Statist. Phys.*, **105**, 353–388, (2001).
39. X.Lu, A modified Boltzmann equation for Bose-Einstein particles: isotropic solutions and long-time behavior, *J. Statist. Phys.*, **98**, 1335–1394, (2000).
40. P. Markowich, L.Pareschi, Fast, conservative and entropic numerical methods for the boson Boltzmann equation, preprint 2002.
41. L. Pareschi, Computational methods and fast algorithms for Boltzmann equations. *Lecture Notes on the discretization of the Boltzmann equation*, ed. N.Bellomo, World Scientific, (2002).
42. L. Pareschi, G. Russo and G. Toscani, Fast spectral methods for the Fokker-Planck-Landau collision operator, *J. Comp. Phys*, **165**, 1–21, (2000).
43. L. Pareschi, G.Toscani and C. Villani, Spectral methods for the non cut-off Boltzmann equation and numerical grazing collision limit, *Numerische Mathematik*, (to appear).
44. L.P. Pitaevskii, *Zh. Eksp. Teor. Fiz.*, **40**, 646, (1961) (*Sov. Phys. JETP*, **13**, 451, (1961)).

45. D.V.Semikoz, I.I.Tkachev, Kinetics of Bose condensation, *Physical Review Letters*, **74**, 3093–3097, (1995).
46. D.V.Semikoz, I.I.Tkachev, Condensation of bosons in the kinetic regime, *Physical Review D*, **55**, 489–502, (1997).
47. G. Strang, On the construction and comparison of difference schemes, *SIAM J. Numer. Anal.* **5**, (1968) pp. 506.
48. J.T.M.Walraven, *Quantum dyanmics of simple systems*, edited by G.L.Oppo, S.L.Burnett, E.Riis and M.Wilkinson, Bristol 1996. (SUSSP Proceedings, vol.44).
49. H. Yoshida, Construction of higher order symplectic integrators, *Phys. Lett. A*, **150**, 262-268, (1990).
50. E.Zaremba, T.Nikuni, A.Griffin, *J. Low Temp. Phys.* 116, p. 277, (1999).